1-1-2019

Amelioration of Alzheimer's Disease Pathology in 12-Month-Old hAPP(SweInd) Transgenic Mice After Treatment with a Cysteine Rich Whey Supplement, Immunocal®

Srivalli Puttagunta
University of Denver

Amelioration of Alzheimer's Disease Pathology in 12-Month-Old hAPP(SweInd) Transgenic Mice After Treatment with a Cysteine Rich Whey Supplement, Immunocal®

Abstract

Deficits in Reelin expression and signaling play a pathogenic role in Alzheimer's disease (AD). Thus, strategies aimed at correcting Reelin deficits may provide a novel therapeutic approach to treating AD. The cysteine-rich, whey protein supplement, Immunocal®, has recently been shown to rescue Reelin expression in a mouse model of Schizophrenia. Given that Reelin-expressing neurons of the entorhinal cortex region are a highly vulnerable population of cells that are lost early in AD, we examined the effects of Immunocal® in the hippocampal-entorhinal cortex formation in a mouse model of AD. Glutathione levels and Reelin expression in the hippocampal-entorhinal cortex formation (entorhinal cortex, EC; dentate gyrus, DG; and Cornu Ammonis, CA1/ Cornu Ammonis, CA3 regions of hippocampus) of 12-month old hAPPSweInd mice were significantly reduced when compared to non-carrier controls as measured by HPLC, western blot and immunohistochemistry respectively. These reductions were prevented in hAPPSweInd mice when treated with Immunocal® from 3 month to 12-month-old. We assessed the transcript levels of Reelin using in situ hybridization and show a reduction in Reelin transcript levels in untreated hAPPSweInd mice compared to non-carrier mice; However, Immunocal® treatment preserved Reelin transcript levels. Elevating Reelin expression through treatment with Immunocal® significantly reduced the number, size and density of Amyloglo stained amyloid plaques throughout the hippocampal-entorhinal cortex formation. Our findings demonstrate that Immunocal® rescues Reelin expression in vivo within the hippocampal-entorhinal cortex formation of 12-month-old transgenic hAPPSweInd mice. This rescue of Reelin expression was associated with an amelioration of the pathological amyloid plaque load. To our knowledge, these data provide the first evidence of a therapeutic agent that is capable of correcting Reelin deficits in the hAPPSweInd mouse model of AD. Our findings support the testing of Immunocal® as a novel therapeutic agent for patients suffering from Alzheimer's disease.

Document Type

Thesis

Degree Name

M.S.

Department

Biological Sciences

First Advisor

Martin Margittai, Ph.D.

Second Advisor

Robert Dores, Ph.D.

Third Advisor

Yan Qin, Ph.D.

Keywords

Aging, Alzheimer's disease, Immunocal, Neurodegeneration, Oxidative stress, Reelin

Amelioration of Alzheimer's Disease Pathology in 12-Month-Old $hAPP_{(SweInd)}$ Transgenic Mice after Treatment with a Cysteine Rich Whey Supplement, Immunocal®

A Thesis

Presented to

the Faculty of Natural Sciences and Mathematics

University of Denver

In Partial Fulfillment

of the Requirements for the Degree

Master of Science

by

Srivalli Puttagunta

August 2019

Advisor: Dr. Daniel Linseman

Author: Srivalli Puttagunta
Title: Amelioration of Alzheimer's Disease Pathology in 12-Month-Old $hAPP_{(SweInd)}$ Transgenic Mice after Treatment with a Cysteine Rich Whey Supplement, Immunocal®
Advisor: Dr. Daniel Linseman
Degree Date: August 2019

Abstract

Deficits in Reelin expression and signaling play a pathogenic role in Alzheimer's disease (AD). Thus, strategies aimed at correcting Reelin deficits may provide a novel therapeutic approach to treating AD. The cysteine-rich, whey protein supplement, Immunocal®, has recently been shown to rescue Reelin expression in a mouse model of Schizophrenia. Given that Reelin-expressing neurons of the entorhinal cortex region are a highly vulnerable population of cells that are lost early in AD, we examined the effects of Immunocal® in the hippocampal-entorhinal cortex formation in a mouse model of AD. Glutathione levels and Reelin expression in the hippocampal-entorhinal cortex formation (entorhinal cortex, EC; dentate gyrus, DG; and Cornu Ammonis, CA1/ Cornu Ammonis, CA3 regions of hippocampus) of 12-month old $hAPP_{SweInd}$ mice were significantly reduced when compared to non-carrier controls as measured by HPLC, western blot and immunohistochemistry respectively. These reductions were prevented in $hAPP_{SweInd}$ mice when treated with Immunocal® from 3 month to 12-month-old. We assessed the transcript levels of Reelin using in situ hybridization and show a reduction in Reelin transcript levels in untreated $hAPP_{SweInd}$ mice compared to non-carrier mice; However, Immunocal® treatment preserved Reelin transcript levels. Elevating Reelin expression through treatment with Immunocal® significantly reduced the number, size and density of Amylo-glo stained amyloid plaques throughout the hippocampal-entorhinal cortex formation. Our findings demonstrate that Immunocal® rescues Reelin expression in vivo within the hippocampal-entorhinal cortex formation of 12-month-old transgenic $hAPP_{SweInd}$ mice. This rescue of Reelin expression was associated with an amelioration of the pathological amyloid plaque load. To our knowledge, these data provide the first evidence of a

therapeutic agent that is capable of correcting Reelin deficits in the $hAPP_{SweInd}$ mouse model of AD. Our findings support the testing of Immunocal® as a novel therapeutic agent for patients suffering from Alzheimer's disease.

Acknowledgments

This is an entirety product of work from this lab which was dedicated with utmost passion. I entered this lab during the latter yet developing stage of reelin project. But, from my very first day until the end of it, I thoroughly enjoyed discussing each prospect of this data. Its always going to be special to me and I hope to be a part of workspace like this in my future endeavors and design projects that resonate with the work presented here.

I have been extremely fortunate to work with my advisor/mentor Dr. Linseman. He pioneered me to take this on with confidence. I couldn't have completed it without his encouragement and having me finish what I've come for. It has been a terrific journey and I cannot thank him enough. I would like to thank my committee members, Dr. Robert Dores and Dr. Yan Qin for comments on this project and steering me in right direction. I would also like to Dr. Martin Margittai, for agreeing to be my committee chair and prompting me to think with very intriguing questions in this project.

I would like to thank everyone's contribution in this project. Alex Sandberg, graduate student and lab manager, for all the mice work, ordering all reagents for the experiments, discussions and editing with thesis. I would like to thank Nathan Duval for all the ideas, performing HPLC and protein staining experiments. Michael Reyna for plaque staining and data analysis. I would like to thank Holly Fleming for western blot data. Undergrads, Kate Heiber and Moriah Mabry, for prep work and behavioral experiments in mice. Lilia Koza for mice colony maintenance and always being my perfect aide to my eventful life. Claudia Pena, for all the suggestions in this project.

Last but not the least I would like to dedicate this work to my parents. I couldn't have done this without their perennial support. I would like to thank Daniel Abbriano for supporting me endlessly and for all advice on my defense presentation.

Table of Contents

List of Figures

Chapter One: Introduction

1.01 Aging and neurodegenerative diseases

Aging is a natural progression of bio-molecular decay that occurs due to entropic events (DiLoreto et al. 2015). This wear and tear originate from cells and eventually translates as a loss of function into tissues and organs. Cellular in-house repair and replacement processes maintain homeostasis such that functional molecules are retained. However, at the cost of reformation some by-products released are often deleterious and non-specific to target. Thereby its effects emerge at a later stage, creating a large asymptomatic period. Consequently, a misbalance in degradation of cellular debris and repair cycle ensues which ultimately results in Age-Related Diseases (ARD). There are several diseases such as cardiovascular, diabetes, neurological diseases that have a time dependency onset. Neurodegenerative diseases make a unique study under ARD since they are elusive in the field of research creating a large rate limiting step towards therapeutics.

Neurodegenerative diseases are a cohort of disorders that cause loss of structure and function in the central and peripheral nervous systems. One of the challenging aspects in this field is drug delivery. This is due to the presence of a blood brain barrier which acts as a molecular sieve wherein selectivity is based on polarity and size. Another complexity of these systems are the maintenance of synapses which assist in transmission of cellular and electrical signaling. Neuronal cells are more susceptible to aging diseases due to lack of regeneration capability once they are terminally

differentiated. Hence, any disruption in synaptic connections that may be the result of deficits in protein synthesis can lead to neuronal death. In order to address these challenges, there is a dire need to understand fundamental processes that are involved in building and maintaining neuronal connections. Alzheimer's disease is one such disease that is a representation of neurodegeneration along the aging process. It currently requires attention due to a growing elderly population that are vulnerable to this form of dementia.

1.02 Prevalence of Alzheimer's disease

Alzheimer's disease (AD) is a chronic illness that is clinically characterized by dementia, behavioral impairment and socio-occupational dysfunction. Dementia is a syndrome that arises due to number of causes and its phenotypic presentation often depends on the severity and area of neuronal degradation. Its typical symptoms present as loss of memory and slow decline of other cognitive functions that affect a person's ability to perform daily activities. As the disease progresses, other areas of the brain begin to degrade that are involved in controlling involuntary activities, making it fatal (Wilson et al. 2012)

Several statistical studies have estimated that approximately 17% of people in the USA between the ages of 75-84 years-old have AD. Due to the nature of AD as being a slow and prolonged debilitating disease, patients often require full attention within caregiver facilities. This has led to greater costs which are estimated at about 236 billion dollars per year. It has been projected that the costs will triple by year 2050. According to the Alzheimer's Association, approximately 13% of people over age 65 have AD and 45% of people over the age of 85 have AD. Due to a better healthcare system overall, there is a larger demographic shift in the population leading to longer lives. Hence it has been predicted that more people may be susceptible to having AD. Based on this predictive analysis, about 7.7 million people are projected to have AD and this number is expected

to double by 2050. AD is the sixth most common cause of death with over 5 million patients currently diagnosed in the United States and approximately 500,000 new cases each year (2017 Alzheimer's disease facts and figures).

1.03 Pathology of Alzheimer's disease and drug interventions

Alzheimer's disease was first described in 1906 by Dr. Alois Alzheimer and is characterized phenotypically by progressive memory loss and cognitive decline (Hanns Hippius, 2003). Pathological hallmarks of the disease include amyloid plaques consisting of insoluble deposits of amyloid beta (Aβ) peptide and neurofibrillary tangles containing hyper-phosphorylated tau protein (Fig 1.) (L.Muche, 2009). These plaques and tangles are found throughout the brain parenchyma and are believed to play a significant role in the neuronal loss and atrophy that are characteristic of the AD brain. Of the diverse neuronal cell types that die in AD, hippocampal pyramidal cells, cortical pyramidal cells, and basal forebrain cholinergic neurons are among the most severely affected. The death of these populations of neurons leads to profound synaptic loss and significant neurotransmitter deficits, particularly in cholinergic pathways (Del Turco, D. et al. 2016) Although 3 genes (amyloid precursor protein (APP), presenilin 1 (PS1), and presenilin 2 (PS2)) have been shown to be mutated in early onset, autosomal dominant, familial AD, these inherited forms of the disease make up less than 5% of AD cases, with the remaining 95% of cases being sporadic in nature (Cacace, R. et al. 2016).

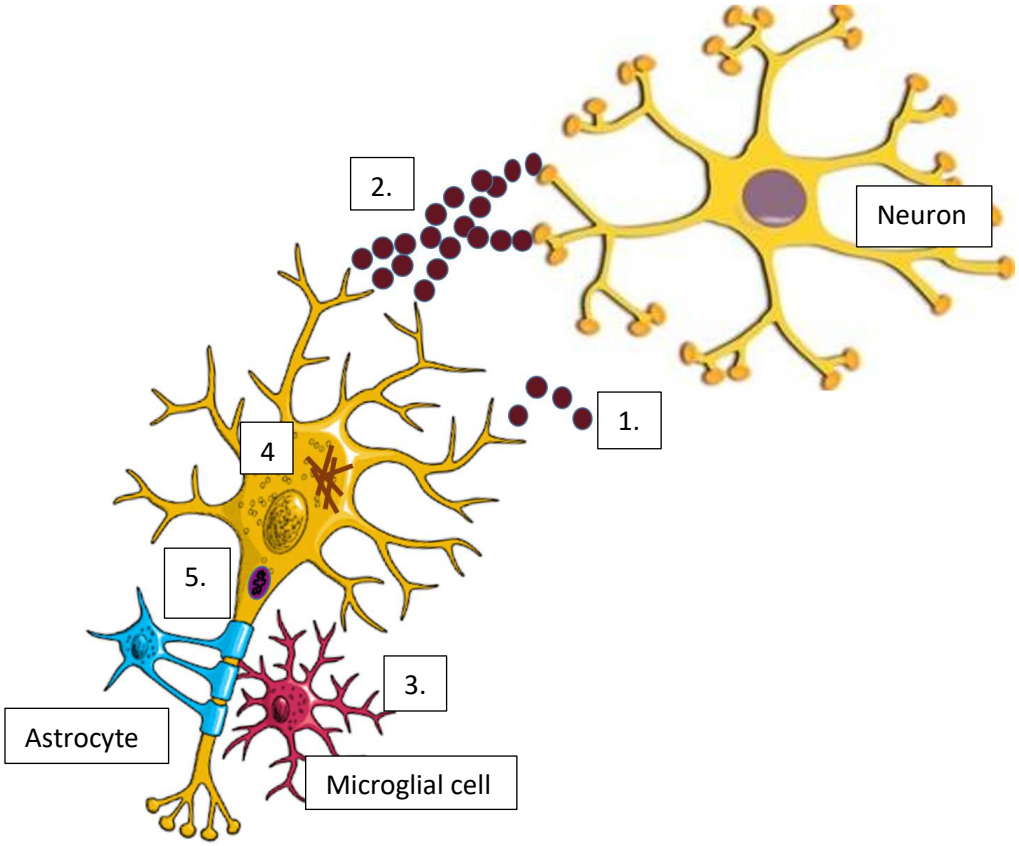

Figure 1: Cellular events of AD pathology (Figure adapted from L.Muche, 2009)

1. Aβ is produced from amyloid precursor protein (APP). They tend to disrupt space between neurons, synapses hindering cell to cell communication
2. Fibrils of amyloid-β oligomers form plaques.
3. Inflammatory response to plaques leads microglial cells to release of cytokines that eventually lead to neuronal death
4. Misfolded tau form fibrils inside the neuron that displace intracellular signaling pathways.
5. Aβ molecule disrupt functions of organelles

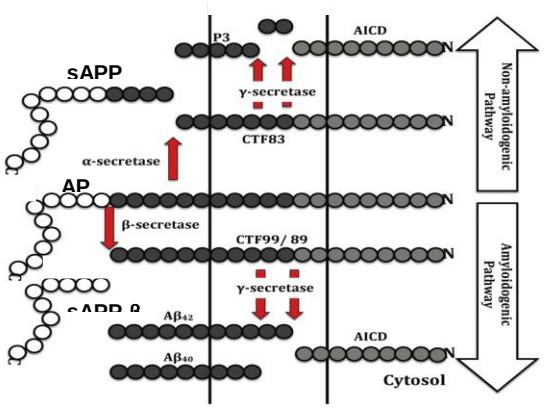

Fig. 2. Distinct pathways of APP proteolytic processing. APP processing has two different pathways once it has been inserted into a lipid membrane. The non-amyloidogenic pathway utilizes α-secretase to produce soluble amyloid-beta precursor protein-alpha ($sAPP_{\alpha}$) and C-terminal fragment 83 (CTF83). γ-secretase then cleaves the CTF83 into a soluble p3 fragment and the amyloid precursor protein intracellular domain (AICD). The amyoidogenic pathway utilizes processing by β-secretase, which produces the soluble amyloid-beta precursor protein-beta ($sAPP_{\beta}$) and C-terminal fragment 99 or 89 (CTF99/89), depending on tissue type. γ-secretase then cleaves CTF99/89 into $A\beta_{40}$ or $A\beta_{42}$, which become extracellular, and the AICD. (Figure adapted from Müller et al. 2008).

The amyloid cascade hypothesis has dominated the field of AD research for the past two decades and is founded on the premise that deposition of Aβ peptide is the initiating event in disease pathogenesis, ultimately leading to neurofibrillary tangle formation, synaptic loss, and neuronal cell demise (Hardy and Higgins, 1992). For nearly two decades, the amyloidogenic processing of APP to form Aβ has been recognized as a viable molecular target for AD therapeutic development (Vassar, 2001; Evin et al. 2006). The amyloidogenic pathway generates beta amyloid (of which the $A\beta_{1\text{-}42}$ form - here referred to simply as Aβ) is commonly regarded as the most likely toxic species) through the sequential cleavage of APP by the beta-site APP cleaving enzyme (BACE; also known as β -secretase) and γ-secretase. Alternatively, the sequential cleavage of APP by α-secretase and γ - secretase is considered non-amyloidogenic (Fig. 2)

Based largely on the amyloid cascade hypothesis (Fig. 3), selective inhibitors of BACE and γ -secretase have been developed as drugs to decrease the tissue load of Aβ in AD brain (Vassar et al., 2009; D'Onofrio et al. 2012). Unfortunately, amyloid altering drugs have resulted in largely disappointing results in the clinic. For instance, two large Phase III clinical trials of the γ -secretase inhibitor, semagacestat, in mild-to-moderate AD

patients were terminated early due to a statistically significant worsening of clinical measures of cognition and ability to perform activities associated with daily living (D'Onofrio et al. 2012). Even more recently, Eli Lilly's anti-amyloid antibody, solanezumab, failed in a Phase III trial of patients with mild-to-moderate AD and a second trial in prodromal AD patients was terminated (Mullard A. 2017). The Merck compound, MK-8931 (verubecestat), is a selective BACE inhibitor that initially completed Phase I testing and reportedly was capable of reducing cerebral spinal fluid amyloid levels by up to 90% in rats, monkeys, healthy human volunteers, and AD patients (Menting and Claassen, 2014; Kennedy M.E. et al. 2016). A Phase II/III clinical trial of this drug (EPOCH) completed enrollment in early 2016 in a population of patients with mild-to-moderate AD. Unfortunately, in February of 2017, Merck announced that it was terminating the trial after an interim analysis suggested little chance of discerning any positive therapeutic benefit (Mullard A. 2017). This was a significant setback for the AD field. As a result of these recent clinical disappointments, and due to the observation that brain amyloid load does not necessarily correlate with the severity of cognitive deficits in AD, some have begun to question whether the amyloid cascade hypothesis is entirely sufficient to explain the underlying pathogenesis of late onset, sporadic AD (Karran and De Strooper, 2016; Swerdlow et al. 2017; Tse and Herrup, 2017). Thus, it is essential to identify novel therapeutic approaches that are not focused exclusively on reducing amyloid load in the AD brain.

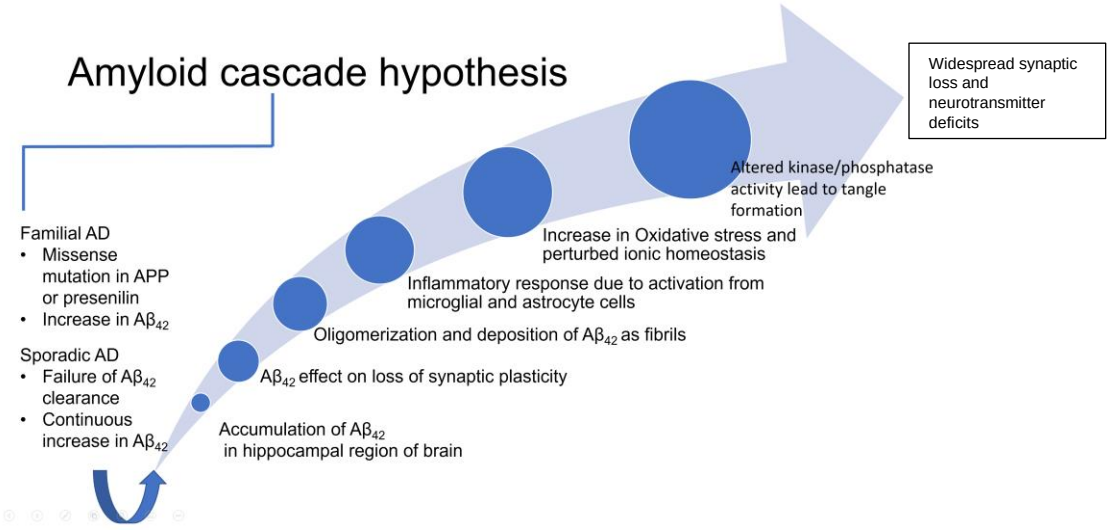

Fig 3. An Illustration of amyloid cascade hypothesis. (Figure adapted from Singh et al. 2016)

1.04 Extracellular secreted protein: Reelin

Reelin may be one such novel approach for AD. It is a large secreted glycoprotein which plays a key role in patterning and layering of the cerebral cortex and other regions of the brain during development (Niu et al. 2004; Beffertt al. 2006; Kim et al. 2015; Bosch et al. 2016). Reelin has specific roles in each developmental phase of the central and peripheral nervous system. This protein was discovered in 1951 as a spontaneous mutation variant in mice which have a typical neurological phenotype of ataxia and “reeling” gait that is an inability to move around the cage (Falcon DS, 1951; Lambert de Rouvroit and Goffinet, 1998). Through chromosome mapping, the reelin gene was found to be present on chromosome 7q22. Later, antibodies were successfully raised against reelin which was termed as CR-50 (Cajal-Retzius 50 marker). During prenatal development Cajal Retzius (CR) are primary cells in the marginal zone that secrete reelin (D’Arcangelo et al. 1997; Ogawa et al. 1995). Failure to form normal cortical plates in the cerebrum and cerebellar hypoplasia are distinct pathological characteristics of reeler mutant mice (Hong et al. 2000). Through this study of histological sections of brain, it was

discovered that reelin plays a significant role in neuronal patterning in the pre-developmental period (Gabriella D'Arcangelo et al.1995). To achieve correct architecture of neocotex, reelin acts as a molecular cue for cells to migrate enabling cells to reach in their destined target area (Fig 4.). These mutants have a severe anatomic defect where all of the layers in the forebrain are disrupted. Shortly after neocortex formation, this population of CR cells die. During the postnatal development phase, residual CR cells are involved in functions like axonal maturation and dendrite outgrowth which provides branching patterns in the brain (Niu et al. 2004; Kupferman et al. 2014). However, in the adult brain only a subset of cells, especially GABAergic interneurons found in cortical, granular layer and hippocampal regions, secrete reelin, and are thought to be involved in synaptic plasticity (Pesold et al. 1998). Therefore, Reelin has myriad roles such as those involved in axonal and dendrite outgrowth, synaptogenesis, spine formation, long term potentiation in developing and post-development phases (Weeber et al. 2002; Beffert et al. 2005). This indicates that it acts on heterogenous cell populations such as glial cells, astrocytes, stem cells, newborn and differentiated cells etc. This spatiotemporal regulation could be attained through various structural conformations of reelin.

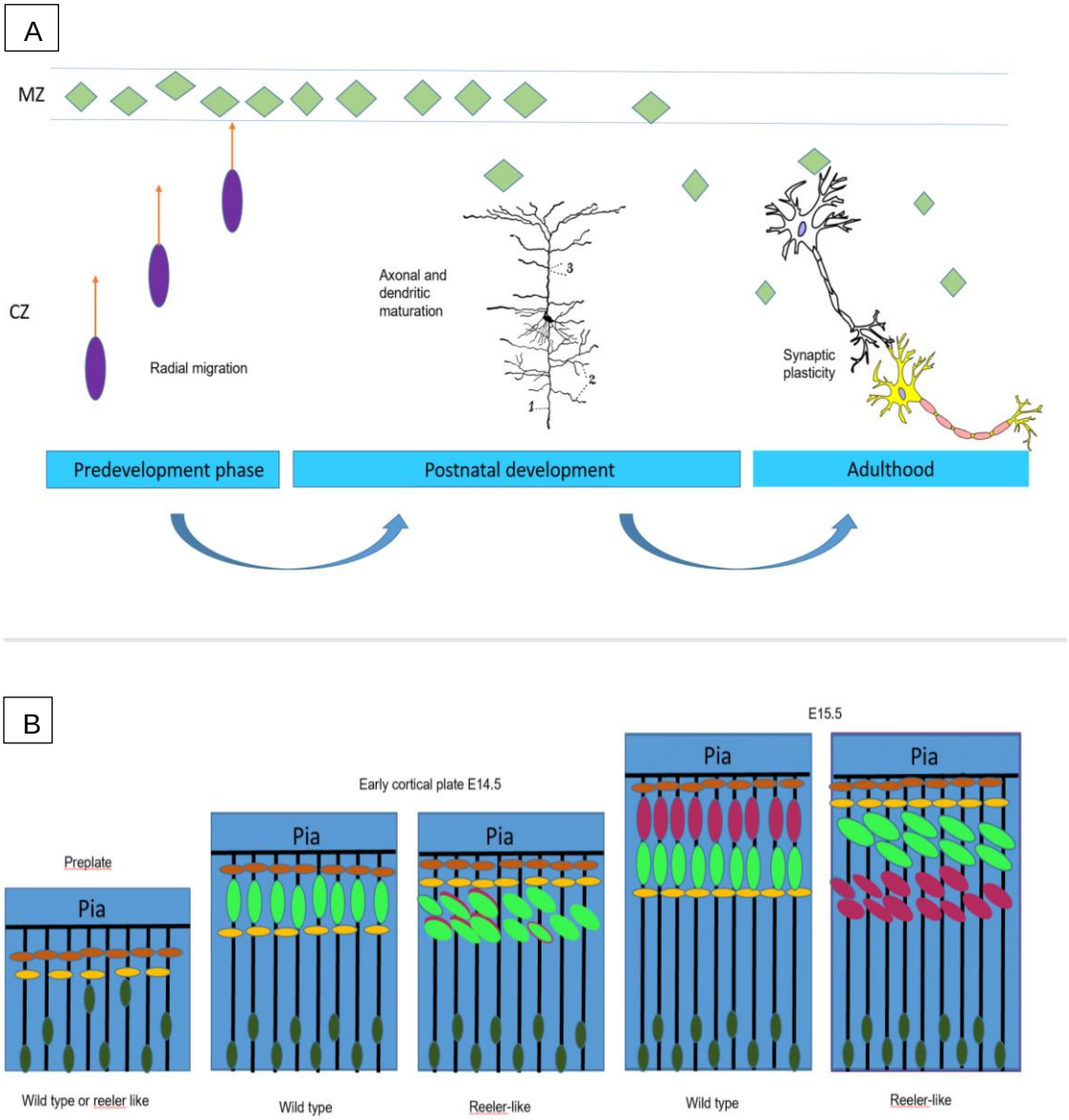

Fig 4. Schematic representation of early cortical development in mice and reelin function in brain development. A) At embryonic day (E) 13.5 (The preplate stage) neurons colonize maybe through somal translocation and form a horizontal trail of cells, as directed by arrows. At this stage reeler phenotype is not distinct from wild type. At E14.5 as embryonic plate complexity increases, cells migrate along the glial fibers. The cells in fluorescent green condense in cortical plate forming two distinct compartments, while in reeler phenotype, same cells are obliquely oriented and does not split the preplate into two compartments. At E15.5, a second group of cells (magenta) migrate through the cortical plate and settle superficially forming an inside to outside gradient. In reeler mutants, these newly formed cohort cells settle in deeper layers of cortex forming an outside to inside gradient. (Adapted from Fadel Tissir 2003)
B)Green squares represent reelin producing cells that are localized in marginal zone (MZ) in predevelopment phase. Purple ovals represent neurnal cell bodies from cortical forebrain (CZ) that migrate towards MZ. In postnatal development, reelin is involved in axonal and dendritic maturation while in adulthood it is involved in maintenance of synaptic plasticity. (Adapted from Gabriella D'Arcangelo 2014).

1.05 Structure of Reelin

Different functional modalities are contributed by distinct structural features of reelin. Human full-length reelin protein is approximately 388 KDa and is composed of eight repeats (R) (Fig. 5). Each of these repeats surround an epidermal growth factor (EGF) like motif. The N-terminus of reelin contains a signal peptide which is structurally like an F-spondin domain while the C-terminal region is positively charged (D'Arcangelo et al.,1997). After secretion, this full-length protein undergoes cleaved by metalloproteases at two sites to create three fragments: an N-terminal (Nt=N-R2), a central(C=R3-R6), and a C-terminal (Ct=R6-CTR) fragment (Koie et al. 2014; Sato et al. 2016). How each fragment or full-length protein is functionally activated and/or regulated is unknown. Although the C-terminal fragment alone was enough for the activation of downstream signaling pathways and cortical pattering in brain slices. From all collective biochemical studies, it seems that fragments of reelin act as regulatory molecules on the full-length protein. At the same time, these fragments also activate signaling pathways that are distant from their source of origin (Jossin et al. 2007).

Since its role is fundamental for neuronal processes like synaptic plasticity, its deficits in reelin expression can lead to severe debilitation of motor or cognitive functions. Several neuropsychiatric disorders such as schizophrenia, autism and depression are associated with a deficit in reelin signaling.

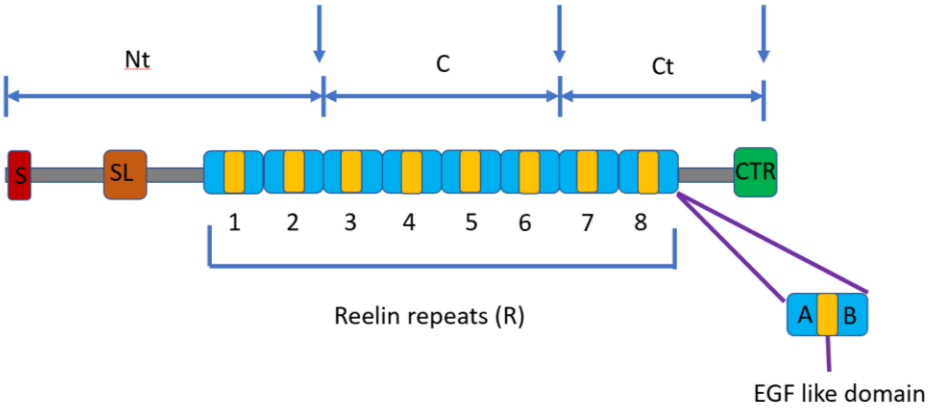

Figure 5. A schematic illustration of reelin protein and its cleavage fragments. Reelin comprises of N-terminal (Nt) signal peptide, F-spondin-like-domain (SL), eight reelin repeats. Each repeat has two subdomains A and B which is separated by epidermal growth factor (EGF). The full-length protein is cleaved at sites shown by an arrow. Figure adapted from Lee (2016).

1.06 Signaling pathway of Reelin

Reelin is secreted into the extracellular space where it interacts with one of two cell surface receptors on target cells, either the very low-density lipoprotein receptor (VLDLR) or the apolipoprotein E receptor-2 (ApoER2) (Fig.6). Upon binding its receptor, Reelin induces tyrosine phosphorylation of the adapter protein, Disabled-1 (DAB1), via the nonreceptor tyrosine kinases, Src or Fyn. Phosphorylated DAB1 acts as a docking site to initiate multiple downstream signal transduction cascades such as those involved in cell survival (PI3K/AKT) and regulation of actin assembly (Cdc42/PAK/cofilin) (Fig. 1; Wasser and Herz, 2017). The pathway described here represents the canonical Reelin signaling pathway and is the one most commonly attributed to Reelin's actions in the central nervous system. However, alternative Reelin signaling pathways do exist, as well as additional Reelin receptors (Bock and May, 2016; Lee and D'Arcangelo, 2016).

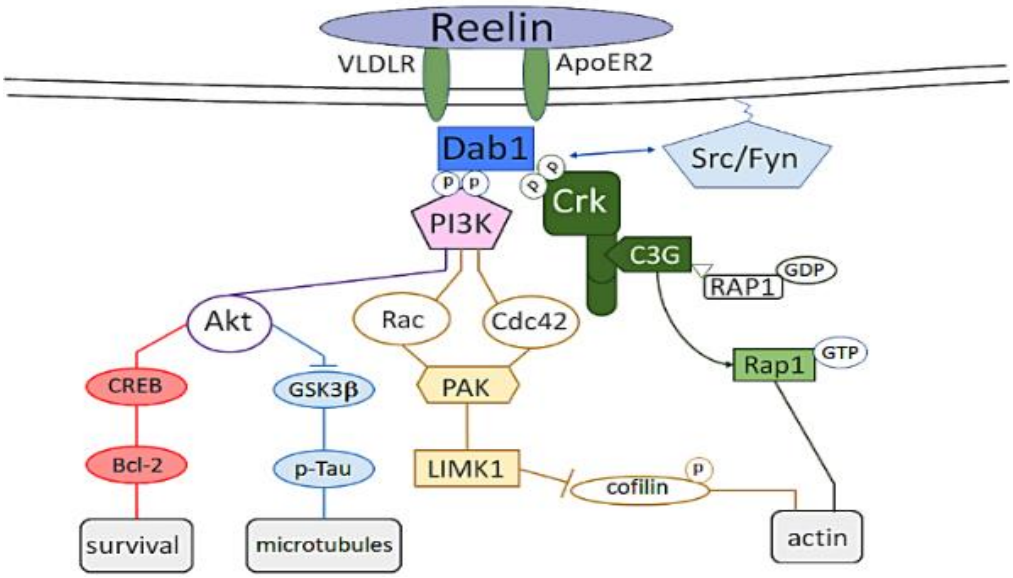

Fig. 6. Canonical Reelin signaling pathway. Reelin binds to one of two cell surface receptors, VLDLR or ApoER2, and induces tyrosine phosphorylation of the adapter protein, Dab1, via Src family kinase activity. Phosphory-lated Dab1 acts as a docking site to initiate multiple downstream signaling cascades. (Figure adapted from Wasser and Herz 2017).

1.07 Non-Canonical receptors of Reelin

Non-canonical pathways refer to Reelin's interaction with cellular receptors other than VLDLR and/or ApoE2, that further lead to activation of Dab1 (Bock, H. H., & May, P. 2016). The core function of Reelin was realized through its interaction with LDL receptors and Fyn-dependent NMDA receptors. NMDA receptors are glutamate receptors that are essential for synaptic plasticity and memory formation. Therefore, Reelin was one of the extracellular proteins that partakes in LTP by consolidating neuronal synapses. Apolioproteins are another class of proteins that interact with LDL receptors. A well-known apolipoprotein variant, ApoE4 has been implicated in sporadic AD. Since the Reelin and ApoE signaling pathways share a common link with LDL receptors, it has been postulated that reelin may be a potential molecule involved in APP processing. It has been shown that reelin levels decrease in an AD mouse model and in AD patients. A novel interaction between reelin and APP has been demonstrated through several in vivo and in-vitro experiments. Overall it was shown that Reelin increases APP receptors on the cell surface

and decreases processing of APP into Aβ peptides. This study also postulates that the interactions of Reelin with APP promotes neurite outgrowth in cultured neurons and dendrite processing in vivo (Hoe, H. S et al., 2009).

1.8 Anatomy of hippocampus

Hippocampus is the region in brain that is predominantly involved with memory and learning. It is composed of three primary regions - dentate gyrus, subiculum and entorhinal cortex (Fig 7.). The dentate gyrus is further subdivided into three parts that are differentiated based on types of cells that populate each part. The molecular layer is a cell-free layer and is composed of apical dendrites that branch in from granular cells. The intermediate layer of DG is also known as the granular layer and consists of a large population of granule cells. Following this layer is the Hilus layer which is distinctively composed of mossy cells. The Cornus Ammonis (CA) is the elongated C shaped structure which is composed of pyramidal cells. This CA region is also sub-divided into three regions, beginning from the region that is at proximity with dentate gyrus, CA3-CA2-CA1 (Amaral, D; Lavenex P;2006). The entorhinal cortex is typically the first region of the brain that is susceptible to plaque deposition and tangle formation in AD.

The major neuronal connections to the hippocampus are through the entorhinal cortex while its major output is through CA1. Neuronal projections in CA1 traverse via two main pathways, that are termed as direct and indirect. The direct pathway involves axons that originate from layer III in EC and form synapses with distal apical dendrites of CA1. The indirect pathway involves axons originating from layer II of EC and finally to CA1 through the trisynaptic circuit. The initial part of this pathway involves axons from the perforant pathway to the granule cells of the dentate gyrus (synapse 1). From there the information follows through the mossy fibers to CA3 (synapse 2). CA3 axons called Schaffer collaterals exit from the cell body and loop around the apical dendrites by

which they connect to CA1 (third synapse). Axons from CA1 then project back to the entorhinal cortex, completing the circuit. In addition to the classical trisynaptic circuitry where CA3 axons connect with CA1 axons, CA3 axons also form collaterals with other CA3 neurons. This recurrent pathway lead to theories of CA3 as forming an auto-associative system of memory (Anderson et al.,2000).

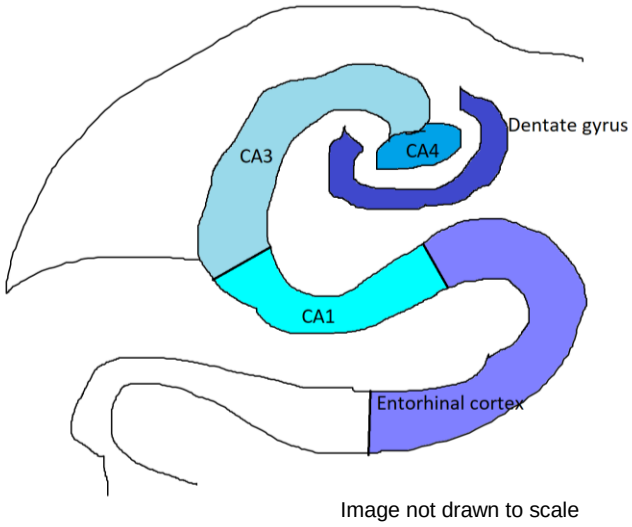

Figure 7: Anatomy of hippocampus in mice.

1.09 Reelin signaling in the entorhinal-hippocampal formation

Neurons of the entorhinal cortex project to the hippocampus and are involved in declarative memory formation and consolidation. Entorhinal cortex layer II neurons provide the principal excitatory input to the dentate gyrus of the hippocampus. The entorhinal cortex layer II neurons are one of the first neuronal populations to die in AD, resulting in a severe loss of synaptic contacts to the dentate gyrus. Many of the entorhinal cortex layer II neurons express Reelin and these Reelin-expressing cells are significantly reduced in the brains of human amyloid precursor protein (hAPP) transgenic mice expressing the Swedish and Indiana mutant form of the hAPP gene ($hAPP_{sweind}$ orJ20 strain). In accordance with the loss of these Reelin-expressing cells, Reelin levels in the

hippocampus of J20 mice are also significantly reduced (Chin et al., 2007). Similar loss of Reelin-expressing entorhinal cortex layer II neurons is also observed in the brains of patients with AD (Chin et al., 2007; Herring, 2012). Finally, in a transgenic rat model of AD (McGill-R-Thy1-APP strain), Reelin-expressing neurons of the entorhinal cortex layer II were found to selectively express increased levels of soluble intracellular Aβ early in disease, prior to the deposition of amyloid plaques (Kobro-Flatmoen, 2016). Collectively, these studies suggest that loss of Reelin-expressing cells and their synaptic projections to the hippocampus play a central role in the early pathogenic changes in AD (Krstic et al., 2013). Moreover, deficiencies in Reelin signaling to the hippocampus likely underlie some of the cognitive deficits observed in patients with AD (Cuchillo-Ibañez et al., 2016; Yu et al., 2016). Therefore, strategies focused on rescuing the deficit in Reelin expression and/or signaling might provide a novel therapeutic approach to treating AD.

1.10 Modulation of Reelin expression in AD alteration

As noted above, Reelin-expressing cells of the entorhinal cortex layer II are significantly reduced in the $hAPP_{SweInd}$ (J20) transgenic mouse model of AD, coinciding with a reduction in Reelin levels in the hippocampus of these mice. Further reducing Reelin in these mice by crossing J20 mice with heterozygous *reeler* mice accelerates amyloid plaque formation and tau pathology (Kocherhans, 2010). Conversely, Reelin over-expression in J20 AD model mice significantly delays amyloid plaque formation and rescues cognitive deficits in these mice (Pujadas, 2014). Thus, J20 mice are an established model of familial AD and the disease course of these mice is significantly impacted by alterations in Reelin, making this an excellent model system to investigate the potential therapeutic benefits of modulating Reelin expression.

1.11 Oxidative stress

Oxidative species are free radical molecules that can arise from exogeneous or endogenous sources (Kim, G. H. et al., 2015). Some of the exogeneous sources are UV radiation, ionizing agents or drugs that have a non-specific mode of action mediated through reactive oxygen species (ROS) production (Mani S. 2015). Endogenous sources of ROS originate from reactions that occur in mitochondria or other non-mitochondrial compartments which are natural by-products of metabolic processes. Some of the enzymes that produce free radicals include nicotinamide adenine dinucleotide phosphate (NADPH) oxidase (Nox), xanthine oxidase (XO), nitric oxide synthase (NOS), cytochrome P450 from endoplasmic reticulum (ER), and flavin oxidases from peroxisomes (Song P et al., 2015). Another source of ROS is through cytokine release from cellular death and tissue injury. Immune neutralization reaction is also involved with a release of oxidative species; reactions such as Antigen Presenting Cells (APC) that are targeted by immune cells. Mitochondrial fission and autophagy are internally programmed mechanism that are activated by cellular sensors from factors such as nutritional starvation or signaling cues that also contribute to oxidative stress.

An excessive production of oxidative species or dysfunction in cellular antioxidant system leads to oxidative stress which has been linked to aging and neurodegenerative diseases. Oxygen tends to form free radicals due to unpaired electrons in its valence shell. Therefore, ROS are a group of derivatives from oxygen molecules (Held P. 2012) Superoxide radicals (O_2•−), hydrogen peroxide (H_2O_2), hydroxyl radicals (•OH), and singlet oxygen ($^1O_2$) are some of the examples of oxidative species. Oxygen radicals are typically short-lived and highly reactive. Hence, they maybe transformed into a stable form such as H_2O_2 by superoxide dismutase or be protonated to form HO^{2-}. H_2O_2can further decompose to form H_2O and O_2 via catalase or peroxidases. Hydroxyl ions are one of the

most reactive species that have cytotoxic effects on cellular components. Hydroxyl ions are also formed from H_2O_2 and O_2 that is catalyzed by Fe ions which are known as Fenton's reaction (Zorov D.B, 2014).

There are physiological benefits of ROS when maintained at low to moderate levels in the cell. Processes such as protein phosphorylation, migration, mitosis, differentiation, immune activation takes place under ROS sensor system. To combat a higher threshold of toxic oxidative species, cells deploy an antioxidant defensive system that are composed of enzymatic components, such as superoxide dismutase (SOD), catalase (CAT), and glutathione peroxidase (GPx) which uses glutathione (GSH) to detoxify peroxides (Kim G.H., 2015). However, in an aged individual, these antioxidant pathways are overwhelmed by ROS.

1.12 Immunocal®: GSH precursor and modulator of Reelin expression

Immunocal® is a non-denatured whey protein isolate and a rich source of the glutathione (GSH) precursor cysteine. Supplements that only contain cysteine are not viable source of glutathione since it is spontaneously catabolized by gastrointestinal tract and blood. However, Immunocal® is metabolized in the liver to form cystine which is resistant to trypsin proteolysis and can pass through the bloodstream. Cystine is transported into neurons via the system xc− antiporter (Sxc−). Cystine is hydrolyzed to form two cysteine molecules, which are then utilized in the de novo synthesis of GSH by γ-glutamylcysteine ligase (γ-GCL) and glutathione synthase (GSS) (Winter et al. 2017).

Glutathione is a tri-peptide (glutamate, cysteine, glycine) endogenous antioxidant. Cysteine and glutamate in presence of enzyme γ-glutamyl synthetase (γ-GCS) forms γ-glutamylcysteine. Glutathione (GSH) is then synthesized from glycine and γ-glutamylcysteine in presence of glutathione synthetase (GS). GSH is further oxidized by neutralizing various free radicals that are produced within the cell. Through kinetic studies,

it has been observed that cysteine is the rate limiting substrate in the synthesis of glutathione. Therefore, Immunocal® may be a potential source to increase cysteine that could lead to a higher conversation rate to glutathione restoring cellular repair from oxidative stress.

The ratio of reduced to oxidised glutathione (GSH:GSSG) within cells is used as a marker of cellular toxicity. Under normal conditions, this ratio is known to be present in mammalian cells in the concentration range of 1–10 mM. However, in a resting cell, the molar GSH:GSSG ratio is found to be greater than 100:1, and in various models of oxidative stress, this ratio has been observed to decrease considerably (Zitka, O. et al. 2012).

Immunocal® has been shown to boost levels of this essential antioxidant and improve muscle strength in certain patient populations, healthy human volunteers, and non-frail elderly subjects (Bounous et al. 1991; Grey et al. 2003). It was previously shown that incubation with Immunocal® protects primary cerebellar granule neurons and various neuronal cell lines from multiple stressors including glutamate, nitric oxide, and Aβ (Winter et al., 2017). Moreover, the neuroprotective effects of Immunocal® observed *in vitro* are dependent on the *de novo* synthesis of GSH. In a similar manner, it was also shown that oral treatment of G93A mutant hSOD1 transgenic mice with Immunocal® preserves spinal cord GSH and delays disease onset in a mouse model of amyotrophic lateral sclerosis (Ross et al. 2014). Finally, in a schizophrenia mouse model characterized by low brain GSH and low Reelin levels, Immunocal® was recently shown to elevate both GSH and Reelin in the brain (Song et al. 2017). In preliminary studies in the Linseman lab, Immunocal® induces Reelin expression in vitro in hippocampal-entorhinal cortex organotypic slices and rescues Reelin expression in vivo in J20 AD model mice at 5-

months of age. Thus, Immunocal® has the capacity to increase brain GSH and in parallel, enhance Reelin expression in both slice culture and mouse models.

Hypothesis**:** We hypothesize that oral treatment with the cysteine-rich whey protein supplement, Immunocal®, from 3-month-old to 12-month-old will significantly rescue GSH levels and Reelin expression in the entorhinal cortex-hippocampus of $hAPP_{sweind}$ mice as well as ameliorate amyloid plaque neuropathology in this mouse model of AD.

1.13 Summary of Major Findings

We evaluated the effects of Immunocal® treatment *in vivo* by treating hemizygous J20 $hAPP_{sweind}$ AD mice from 3 months-old to 12 months-old. We assessed Reelin expression by western blotting and immunofluorescence microscopy. Immunocal® treatment corrected a deficit in cortical GSH levels observed in the brains of untreated hemizygous J20 mice. Western blotting of brain sections micro-dissected to enrich for the hippocampal-entorhinal cortex sub-region revealed a decrease in Reelin expression in untreated hemizygous J20 AD mice compared to non-carrier control mice. These deficits were corrected by treatment with Immunocal®. In a similar manner, using immunofluorescence microscopy, Reelin expression was diminished in the entorhinal cortex, dentate gyrus and CA1/CA3 regions of the hippocampus in untreated hemizygous J20 AD mice compared to non-carrier control mice. In contrast, Immunocal® treatment rescued these deficits in Reelin expression. Since reelin protein is ubiquitously produced in all regions of the brain, we analyzed reelin transcripts in hippocampal region of J20 AD mice by in situ hybridization. We found that reelin mRNA levels were significantly reduced in entorhinal cortex region of hippocampus and this deficit was also rescued by treatment with Immunocal®. In parallel with the observed rescue of Reelin expression in the hippocampus-entorhinal cortex of J20 mice, Immunocal® also preserved GAD67 expression in the dentate gyrus and CA3 region of the hippocampus. Perhaps most

importantly in the context of AD, we evaluated the deposition of amyloid plaques in the J20 mice. These mice have been shown to have significant plaque load at 12-months-old. We show that untreated J20 mice do indeed accumulate a significant plaque load in the hippocampus and entorhinal cortex. After treatment with Immunocal® the plaque load was diminished quite dramatically, both in size and number.

Chapter Two: Materials and Methods

2.01 Reagents

Immunocal® was provided by Immunotech (Vaudreuil-Dorion, QC, CA). Gey's balanced salt solution and ProLong Gold was purchased from Invitrogen (Carlsbad, CA, US). Primary antibodies for Reelin (ab78540), NeuN (ab104225), DRAQ7™, and β-actin (ab 115777) were purchased from Abcam (Cambridge, UK). Secondary antibodies for immunofluorescence were purchased from Jackson Immunoreserach (Westgrove, PA, US). Horseradish peroxidase (HRP) secondary antibodies for Western blotting were purchased from Bio-Rad, catalogue no. 1706515 (Hercules, CA, US). All probes (RNAscope® Probe Mm-Reln-C3 catalogue no. 319361-C3) and reagents (RNAscope® fluorescent multiplex kit, catalogue no.320850) for in situ hybridization were purchased from Advanced Cell Diagnostics (Newark, CA, US). Amylo-Glo was purchased from Biosensis (Thebarton, SA, AU).

2.02 Experimental model:

To investigate the effects of Immunocal® on Reelin expression *in vivo*, we utilized the hAPP(Swe/Ind) mutant transgenic mouse model of AD (J20 strain). This mouse model is commercially available from Jackson Laboratories (B6.Cg-Tg(PDGFB-APPSwInd) 20Lms/2Mmjax) and displays significant brain pathology, amyloid plaques, and cognitive deficits that recapitulates multiple aspects of AD in humans (Mucke et al., 2000; Karl et al., 2012; Diaz-Hernandez et al., 2012). According to previous reports, these transgenic mice typically show significant cognitive deficits, diminished numbers of Reelin-positive,

entorhinal cortex (EC) layer II neurons, and decreased Reelin expression in the hippocampus by approximately 4-5 months of age. Above, in concordance with the literature, we demonstrated that these mice show deficits in GSH, elevated oxidative stress, and reduced levels of Reelin protein in the hippocampal-entorhinal cortex formation at 5-months of age. As these mice age, amyloid plaques (a hallmark of AD pathology) are visible in the brains of these mice by around 12-months of age. All animal studies were conducted in accordance with a protocol approved by the University of Denver Institutional Animal Care and Use Committee.

2.03 Immunocal® treatment:

To address this experimental question required three groups of mice: hAPP(Swe/Ind) mutant hemizygous mice (J20 strain) treated with Immunocal® (3.3% w/v in drinking water *ad libitum*, as previously described by Ross et al., 2014), untreated hemizygous J20 mice, and untreated non-transgenic (non-carrier) control mice. Immunocal® treatment was initiated at 3-months-old and continued until the mice were 12-months-old.

2.04 Analysis of brain GSH and GSSG by HPLC with electrochemical detection (HPLC-ECD)

2.041 Tissue processing:

Cortical tissue was obtained from mice and immediately frozen in liquid nitrogen. For HPLC-ECD analysis, 2.5M perchloric acid was added and the brains were roughly chopped using pointed surgical scissors. Samples were then sonicated 3 times for 15s intervals. Samples were then centrifuged for 5min at 13,000rpm and the supernatant was removed. A 20µL aliquot of the supernatant was used for a BCA protein assay. The remainder of each solution was neutralized with 500µL of 4M KOH and vortexed

thoroughly. Samples were then centrifuged for 15min at 13,000rpm, and stored at -80°C until separation and analysis by HPLC-ECD.

2.042 HPLC-ECD:

GSH in samples and known standards were separated by reversed-phase HPLC on a C18 bonded silica column at 35°C (5µm, 4.6mm x 25cm) from Tosoh Bioscience. (Grove City, OH, US). Analytes were detected using a CoulArray® detector (model 5600, ESA) on three coulometric array cells in series; electrochemical detectors were set between 0 and 900mV at increments of 75mV. Concentrations were determined with a standard curve of each identified analyte. Mobile phase consisted of 50mM lithium acetate and 1% acetonitrile in water, pH 3.8. The flow rate was set to 0.4mL/min for all samples. CoulArray® software was used for baseline correction and peak analysis.

2.05 Western Blotting

Mice brain was rapidly dissected where one hemisphere was placed into ice cold Gey's balanced salt solution for slicing–while the other half was flash frozen in liquid nitrogen and stored at -80^{0}C. Briefly, the flash frozen half were thawed, then brain slices were lysed using a Dounce homogenizer and Wahl lysis buffer supplemented with aprotinin and leupeptin. The samples were diluted 1:100 for a BCA protein assay. Western immunoblotting was done to immunochemically detect proteins immobilized on polyvinylidene difluoride (PVDF) membranes. Protein samples (50 µg/lane) were resolved by SDS-PAGE and proteins were then transferred to PVDF membranes. Non-specific binding sites were blocked using 1% BSA in PBS (pH 7.4) containing 0.1% Tween-20 (PBS-T) for 1 h at 25°C. The blocking buffer was drained, and the membrane was allowed to incubate in primary Reelin antibody (1:1000) diluted in blocking buffer overnight at 4 °C. The membrane was washed 3 times for 15min in PBS-T. Immunoreactive proteins were detected using enhanced chemiluminescence (GE Healthcare; Pittsburgh, PA) and films

were developed using a ChemiDoc developer (BioRad, Hercules, CA). Re-probing of blots was performed by stripping in 0.1 M Tris-HCl (pH 8.0), 2% SDS, and 100 mM β-mercaptoethanol for 30min at 52 °C. The blots were rinsed twice in PBS-T and processed as above with a different primary antibody. Relative intensities of the protein bands were quantified by scanning densitometry using ImageJ.

2.06 Insitu mRNA Hybridization

Samples were processed according to ACD RNAscope Fluorescent Multiplex Assay manual (Newark, CA, US). Using a vibratome (Leica), brain tissue was freshly sliced in ice cold Gey's balanced salt solution at (roughly 500 µM thickness) such that the hippocampal entorhinal cortex region was preserved, then the slices were embedded in OCT and frozen in liquid nitrogen. Brains were then sliced at 30µm thickness with a cryostat (Leica CM 1950) and adhered onto SuperFrost Plus Slides and stored at -80^{0}C until use. Sliced tissues were permeabilized using 4% paraformaldehyde (PFA) and incubated for 15min. Slides were rinsed twice with 1X PBS (pH 7.4) buffer. Tissues were dehydrated consecutively in 50%, 70% and 100% ethanol for 2min each. A barrier was created around the tissue using a hydrophobic pen. Tissues were then incubated in protease inhibitor for 30min at 25°C in HybEZ™ Humidity Control Tray. About 4-6 drops of Reelin or NeuN (positive control) probe was added to tissues. The slides were inserted in slide holder and placed in HybEZ™ Humidity Control Tray and incubated for 2h at 40^{0}C in HybEZ™ Oven. After washing in 1X PBS buffer, samples were hybridized by adding 4-6 drops with Amp1, Amp2 and Amp3 for 30, 15, 30min respectively at 40^{0}C. Samples were incubated with FITC dye for 15min at 25°C and counter stain DRAQ™ was added for 15min.

2.07 Immunofluorescence

Using a vibratome (Leica), brain tissue was freshly sliced in ice cold Gey's balanced salt solution at (200μM thickness) such that the hippocampal entorhinal cortex region was preserved, then was added to a 6-well plate (1 slice/well) containing ice cold 4% PFA and fixed for 90min. Fixative was removed from the wells and the slices were washed three times for 5min in PBS-T. After the final wash, PBS-T was removed and 1ml of Blocking Solution (5% BSA, 1× PBS, 0.05% Tween-20, pH 7.4) was added to the wells and incubated at 25°C for 90min. Blocking solution was replaced with primary antibody in blocking solution at the specified dilutions. (Table 1) and incubated overnight at 4^0C. The following day, primary antibody was removed, and the tissue was washed 3 times for 5min in PBS-T. Slices were then incubated with the secondary antibody diluted in blocking solution at the indicated concentrations for 90min at 25°C. Then, secondary antibody solution was removed and immediately replaced with 1ml of DRAQ7™ diluted in PBS-T and incubated for 20min at 25°C. The tissue was carefully transferred to a glass slide SuperFrost Plus Slide and excess PBS-T was removed using a Kimwipe Prolong Gold was added onto the tissue and coverslip was placed over it.

Table 1: Antibody concentration and stains

Primary Antibody	Host	Dilution
Reelin (RELN)	Monoclonal mouse anti reelin	1:1000
GAD67	Monoclonal mouse anti GAD67	1:1000
NeuN	Rabbit polyclonal anti NeunN	1:1000
Secondary antibody	**Host**	**Dilution**
Fluorescein Isothiocyanate (FITC) conjugated	anti-goat/rabbit/mouse depending on the primary	1:5000
Cyanine-3 (Cy3) conjugated	anti-goat/rabbit/mouse depending on the primary	1:5000
HRP conjugated	Goat anti-mouse HRP	1:5000
Stains		
DRAQ7™	Nuclear specific stain	1:1000
Amylo-Glo®	Aβ plaque specific stain	1:100

2.08 Quantification of reelin staining and amyloid plaques

Images were collected using Olympus FLUOVIEW FV3000 confocal laser scanning microscopy using an Olympus 20X PLN objective. Confocal z-series were captured at same exposure times across all samples (n=4 to 5 in each group for protein staining and n=3 in in situ hybridization). Each region of hippocampus (EC, DG, CA3/CA1) was captured in triplicates. Total fluorescent intensity was analyzed in Adobe Photoshop for protein staining and in situ hybridization. Any adjustments made in the analysis step was accounted constant for all the groups.

For amyloid quantification by image J software, the color images were converted in to HSV format and 8-bit channels. Plaques were quantified in an unbiased manner by an investigator blind to the treatment nature of the samples. Plaque number was calculated from each area of hippocampus whereas plaque load was calculated as the area occupied by the plaques divided by the total brain region area.

2.09 Statistical analysis

All the data collected were analyzed with GraphPad Prism 5 software using one-way analysis of variance (ANOVA) followed by a post-hoc Tukey's test. Descriptive statistics were displayed as an expressed mean ± S.E.M. Quantitative differences were deemed significant when $p < 0.05$.

Chapter Three: Results

3.01 Glutathione Analysis

We measured the brain levels of reduced glutathione (GSH) and oxidized glutathione disulfide (GSSG) in cortical tissue from the mice using HPLC-ECD. Untreated hemizygous J20 mice displayed a reduction in cortical GSH and a dramatic increase in GSSG at 12-months-old when compared to non-carrier control mice (Fig. 8 A, B). Hemizygous J20 mice treated with Immunocal® showed a complete preservation of cortical GSH and a reduction in GSSG, both of which were statistically significantly different from the levels observed in untreated hemizygous mice (Fig. 8 A, B). Furthermore, the GSH/GSSG ratio, a key measure of oxidative stress, showed a statistically significant reduction in the untreated hemizygous mice when compared to the non-carrier control mice (Fig. 8 C). This indicates increased oxidative stress in the brain of J20 AD mice. This effect was completely prevented by treatment with Immunocal® from 3-months-old to 12-months-old (Fig. 8C). Therefore, Immunocal® treatment corrects a deficit in brain GSH, reduces levels of GSSG, and diminishes the abnormal levels of oxidative stress as indicated by the GSH to GSSG ratio observed in AD model mice.

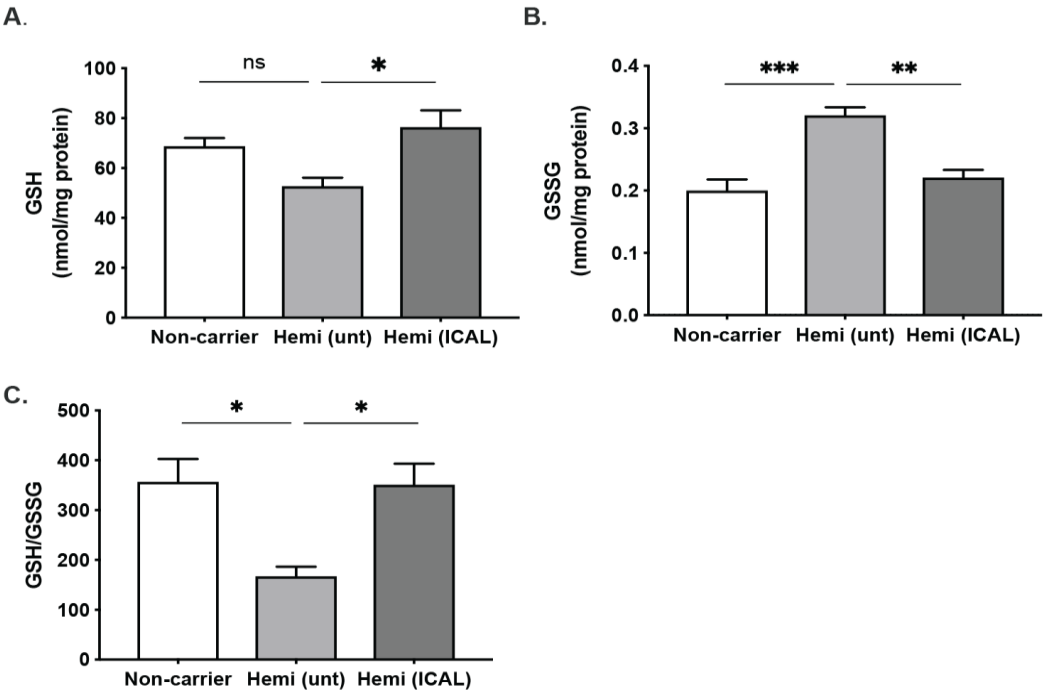

Fig. 8. Immunocal® treatment preserves brain GSH in J20 AD model mice. Brain (cortical) tissue was harvested from 12-month-old hemizygous J20 AD mice (either untreated (Unt) or treated with Immunocal® (ICAL) for 2 months and non-carrier control mice. Tissue was extracted and reduced GSH and glutathione disulfide (GSSG) were measured by HPLC with electrochemical detection. Values are normalized to protein content represented as mean±SEM for n=3 mice per group. Statistical differences were calculated by one-way ANOVA with a post hoc Tukey's test. ns=not significant, *p<0.05, **p<0.01, ***p<0.001.

3.02 In situ mRNA Hybridization for reelin transcript

We used in situ hybridization technique to analyze regions of hippocampus that express reelin transcripts. Entorhinal cortex (EC) is a primary region in hippocampus to produce reelin. Along with EC, interneurons also synthesize reelin in the CA3 region. In this study, we found mRNA expression for reelin mostly concentrated in the regions of hilus layer in dentate gyrus, CA3 and entorhinal cortex of hippocampus. We compared regions of entorhinal cortex and CA3 of non-carrier with hemizygous untreated and Immunocal® J20 mice. There was a significant decrease in reelin transcript levels detected in CA3 and EC regions of hemizygous untreated mice when compared to non-carrier. Immunocal® treatment significantly preserved reelin transcript expression only in the EC (Fig. 9 A,B).

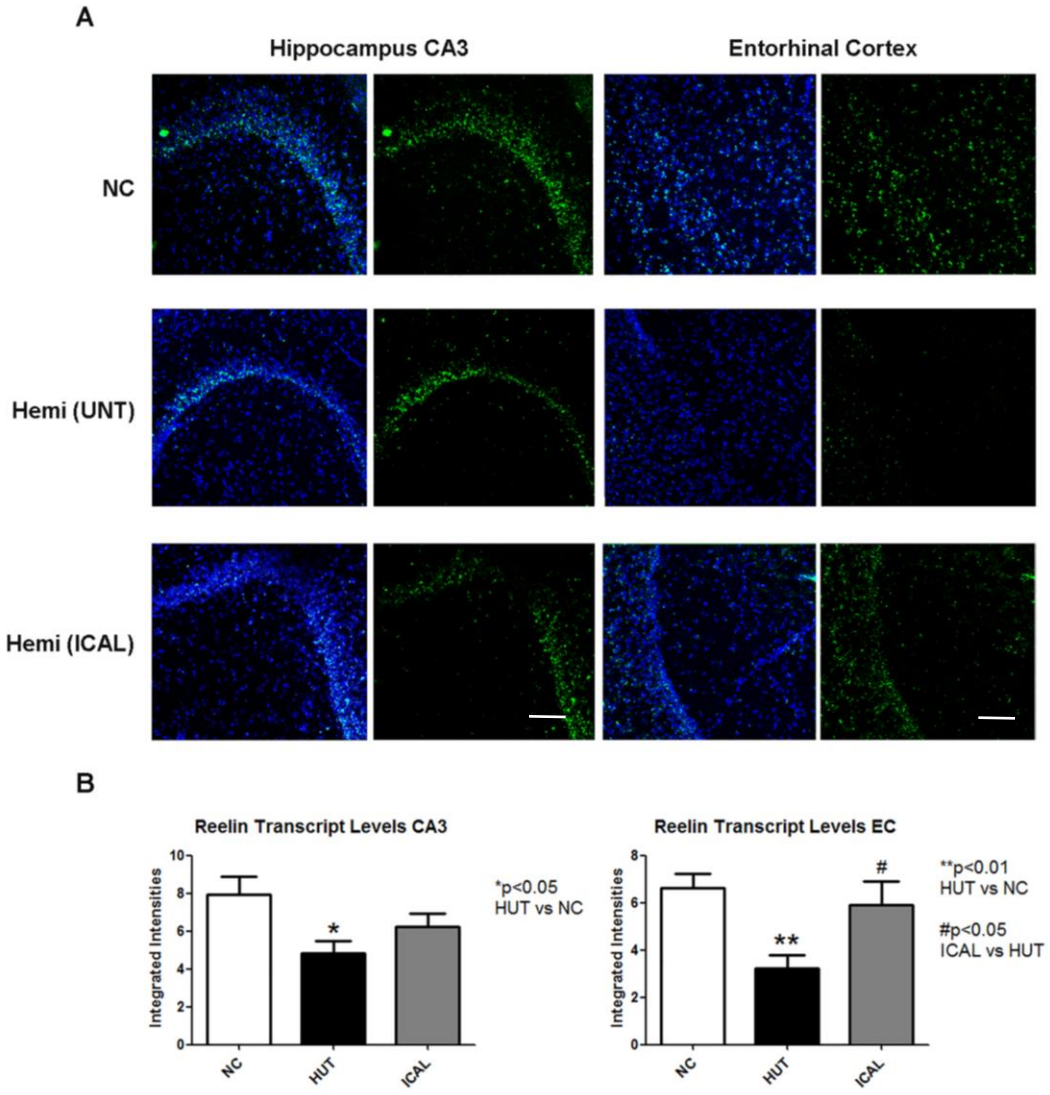

Fig. 9. Immunocal® treatment increases Reelin mRNA expression in hippocampal-entorhinal cortex slices. (A) Brain tissue was harvested from 12-month-old hemizygous (Hemi) J20 AD mice (either untreated (Unt) or treated with Immunocal® (ICAL) for 9 months) and non-carrier control mice. Formalin-fixed sections were hybridized with anti-sense Reelin transcript (Rln, shown in green) along with Draq (nuclear stain, shown in blue). Scale bar = 250µm

(B) The graph indicates total fluorescent intensities for (n = 3) mice in CA3 and EC region of hippocampus. Reelin was significantly decreased in CA3 and EC in untreated hemizygous mice compared to non-transgenic controls. ICAL treatment significantly preserved Reelin staining in the hemizygous mice only in EC. Statistical differences were calculated by one-way ANOVA with a post hoc Tukey's test.

3.03 Analysis of Reelin Expression – Western Blotting

We next evaluated the expression of Reelin protein in the 12-month-old J20 AD mice by western blotting brain tissues enriched for the hippocampal-entorhinal cortex formation. Reelin expression was significantly reduced in untreated hemizygous J20 AD mice compared to non-carrier controls and Immunocal® treatment largely corrected this deficiency (Fig. 10A). The Reelin blots were stripped and re-probed for beta-actin as a loading control. We detected the 180 kDa cleavage fragment of Reelin in these mouse brain lysates. Quantitative densitometric analysis of the 180 kDa Reelin band (normalized to β-actin) revealed an approximate 30% reduction in Reelin protein expression in hemizygous untreated AD mice compared to non-carrier controls, and a complete preservation of Reelin expression in Immunocal®-treated mice (Fig. 10B). In concordance with the literature, we show a reduction in the Reelin protein levels by western blot in 12-month-old J20 AD mice. We also show that treatment with Immunocal® rescues this Reelin deficit in the hippocampal-entorhinal cortex formation

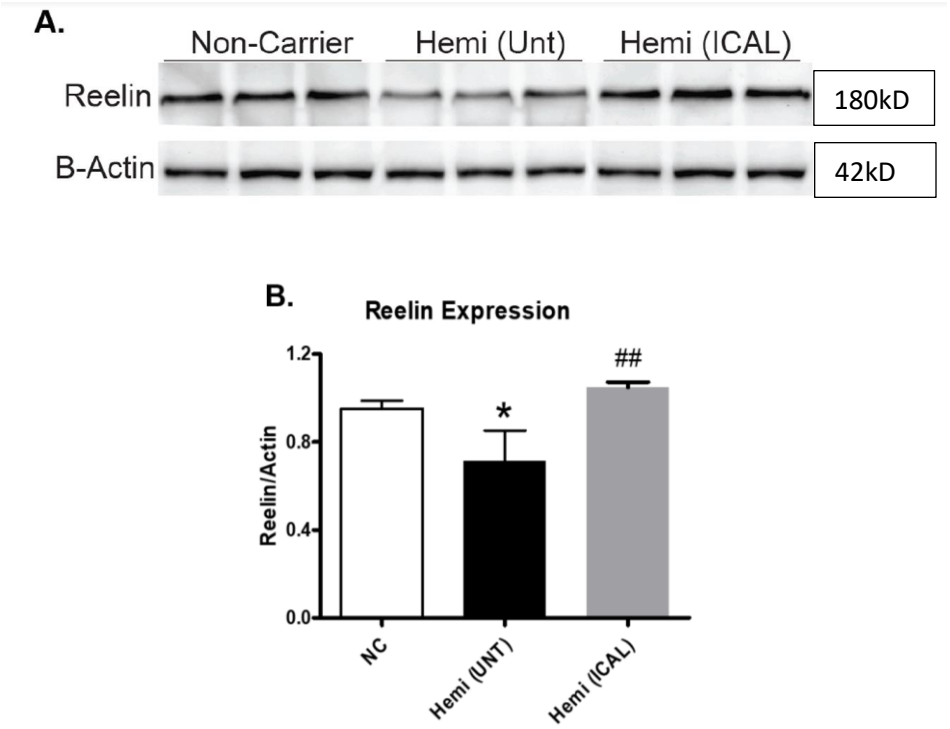

Fig 10. Immunocal® treatment rescues Reelin expression by western blotting in J20 AD model mice. Brain tissue was harvested from 12-month-old hemizygous (Hemi) J20 AD mice (either untreated (Unt) or treated with Immunocal® (ICAL) for 9 months) and non-carrier control mice. Tissue was micro-dissected to enrich for the hippocampal-entorhinal cortex sub-region. (A) Brain lysates were resolved by SDS-PAGE and immunoblotted for Reelin. The Reelin blot was stripped and re-probed for beta-actin. (B) The graph shows the densitometric analysis of the 180 kDa Reelin bands normalized to the beta-actin bands in arbitrary units (n=3 mice per group). Statistical differences were calculated by one-way ANOVA with a post hoc Tukey's test. *p<0.05.

3.04 Analysis of Reelin Expression – IHC

We then used IHC and immunofluorescence microscopy technique to evaluate eelin expression in the entorhinal cortex, dentate gyrus, and CA1/CA3 regions of the hippocampus in 12-month-old J20 AD model mice. In comparison to the non-carrier control, untreated hemizygous J20 AD mice displayed a significant reduction in Reelin immunoreactivity in all the regions of hippocampus. Intriguingly, treatment with Immunocal® from 3 months-old to 12 months-old largely rescued this deficit in Reelin expression within dentate gyrus and entorhinal cortex region of J20 AD mice (Fig. 11 A-D).

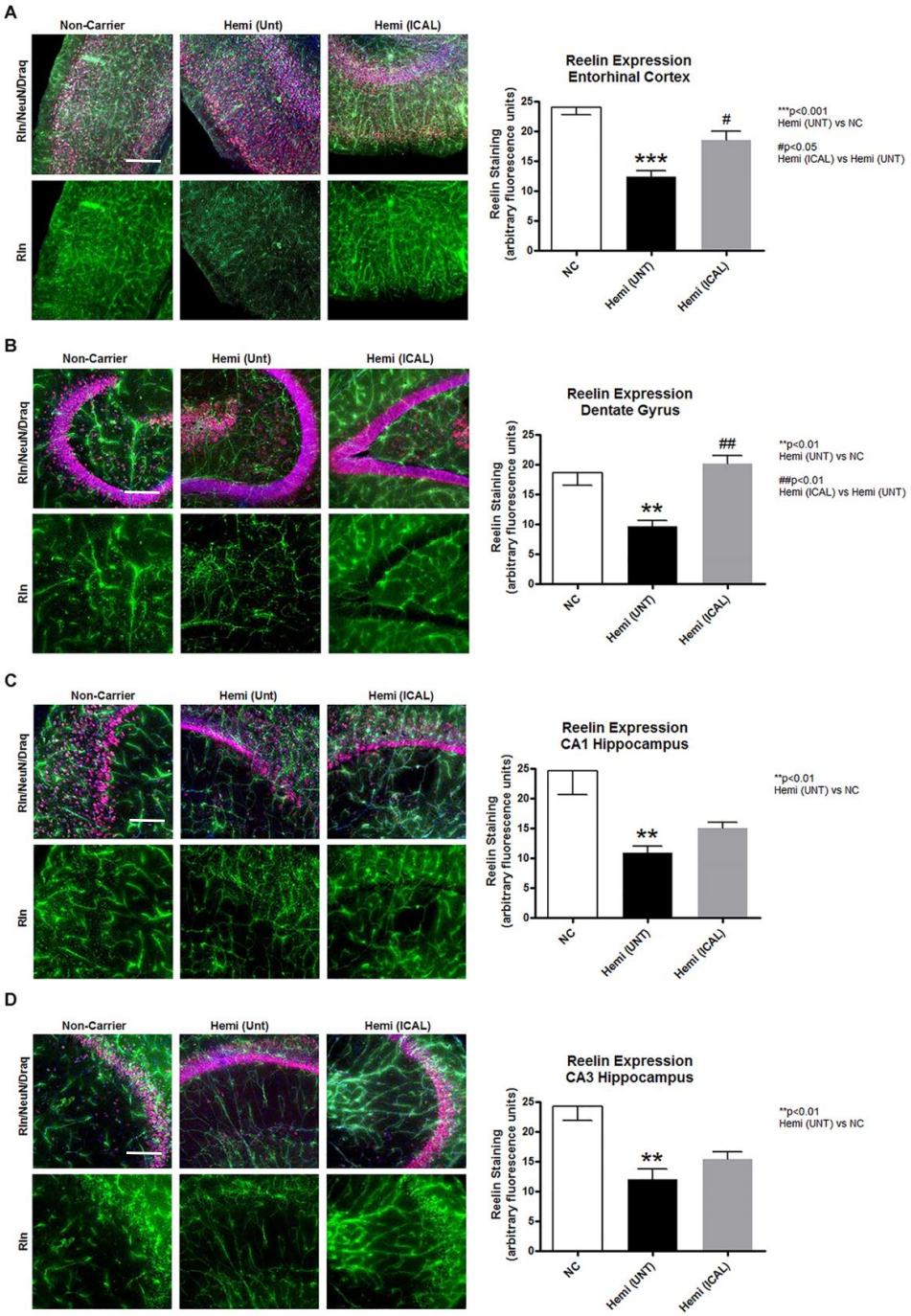

Fig 11. Immunocal® treatment rescues Reelin expression by Immunohistochemistry in J20 AD model mice. Brain tissue was harvested from 12-month-old hemizygous (Hemi) J20 AD mice (either untreated (Unt) or treated with Immunocal® (ICAL) for 9 months) and non-carrier control mice. Formalin-fixed sections were co-stained with antibodies to Reelin (Rln, shown in green) and NeuN (shown in red), along with Draq (nuclear stain, shown in blue). Scale bar = 250μm

The graph indicates total fluorescent intensities for (n = 4-5) mice in each region of the hippocampus. Reelin was significantly decreased in (A)EC, (B)DG, (C)CA1, and (D)CA3 in untreated hemizygous mice compared to non-transgenic controls. In the EC and DG, ICAL treatment significantly preserved Reelin staining in the hemizygous mice. Statistical differences were calculated by one-way ANOVA with a post hoc Tukey's test.

3.05 Analysis of Amyloid plaque load

The J20 mice have been shown to have extensive amyloid-beta plaque loads in the hippocampal entorhinal cortex formation by 12-months of age. To evaluate the effects of Immunocal® treatment on the deposition of amyloid plaques we used Amylo-glo, an amyloid peptide aggregate-specific stain used to mark amyloid plaques. After treating the mice from 3-months-old to 12-months-old with Immunocal® there was a dramatic reduction in the amyloid plaque load in the hippocampal entorhinal cortex formation of the J20 mice (Fig. 12). In the dentate gyrus, CA3 and CA1 hippocampal regions of untreated J20 mice there was a significant plaque load throughout with distinct dense formations (Fig. 12). After treatment with Immunocal® for 9-months, this plaque load was greatly diminished in the hippocampus and the plaques that are visible are much smaller in diameter and density (Fig. 12). When we evaluated the entorhinal cortex of untreated J20 mice we show a similar number of plaques, however a reduced size and density of amyloid-beta plaques relative to the hippocampus. The Immunocal® treated mice have diminished size and density of amyloid plaques in the entorhinal cortex (Fig. 12). We quantified the total plaque number and total plaque load (plaques/area) and show significant reductions in all areas of the hippocampus and entorhinal cortex, with the exceptions of CA3 which shows a trend towards significance (Fig. 13 A, B). These data show the ability of Immunocal® treatment to suppress and delay the formation of amyloid plaques in the hippocampus and entorhinal cortex of the J20 mouse model of AD.

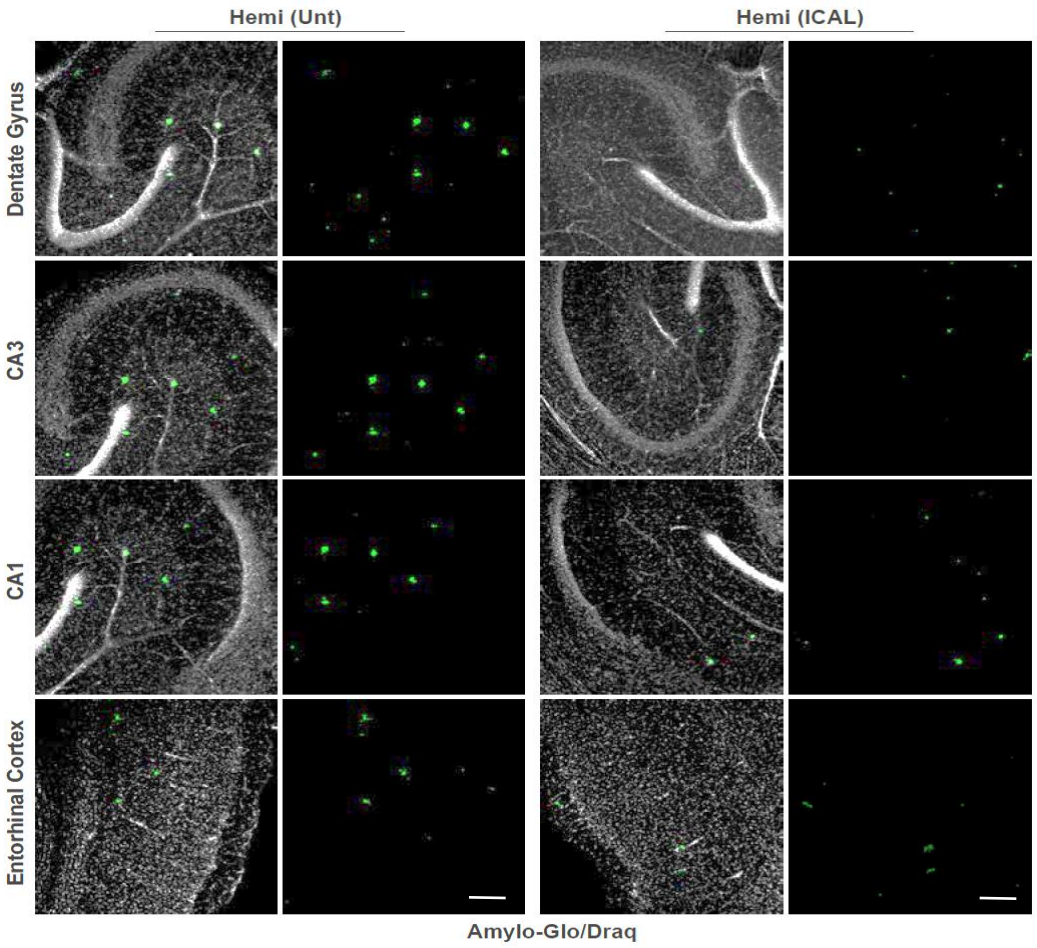

Fig 12. Immunocal® treatment reduces amyloid-beta plaque load in the hippocampal-entorhinal cortex of J20 AD model mice. Brain tissue was harvested from 12-month-old hemizygous (Hemi) J20 AD mice (either untreated (Unt) or treated with Immunocal® (ICAL) for 9 months). Formalin-fixed sections were co-stained with Amylo-glo (amyloid peptide aggregates) in green along with Draq (nuclear stain, shown in grey scale) Scale = 500µm

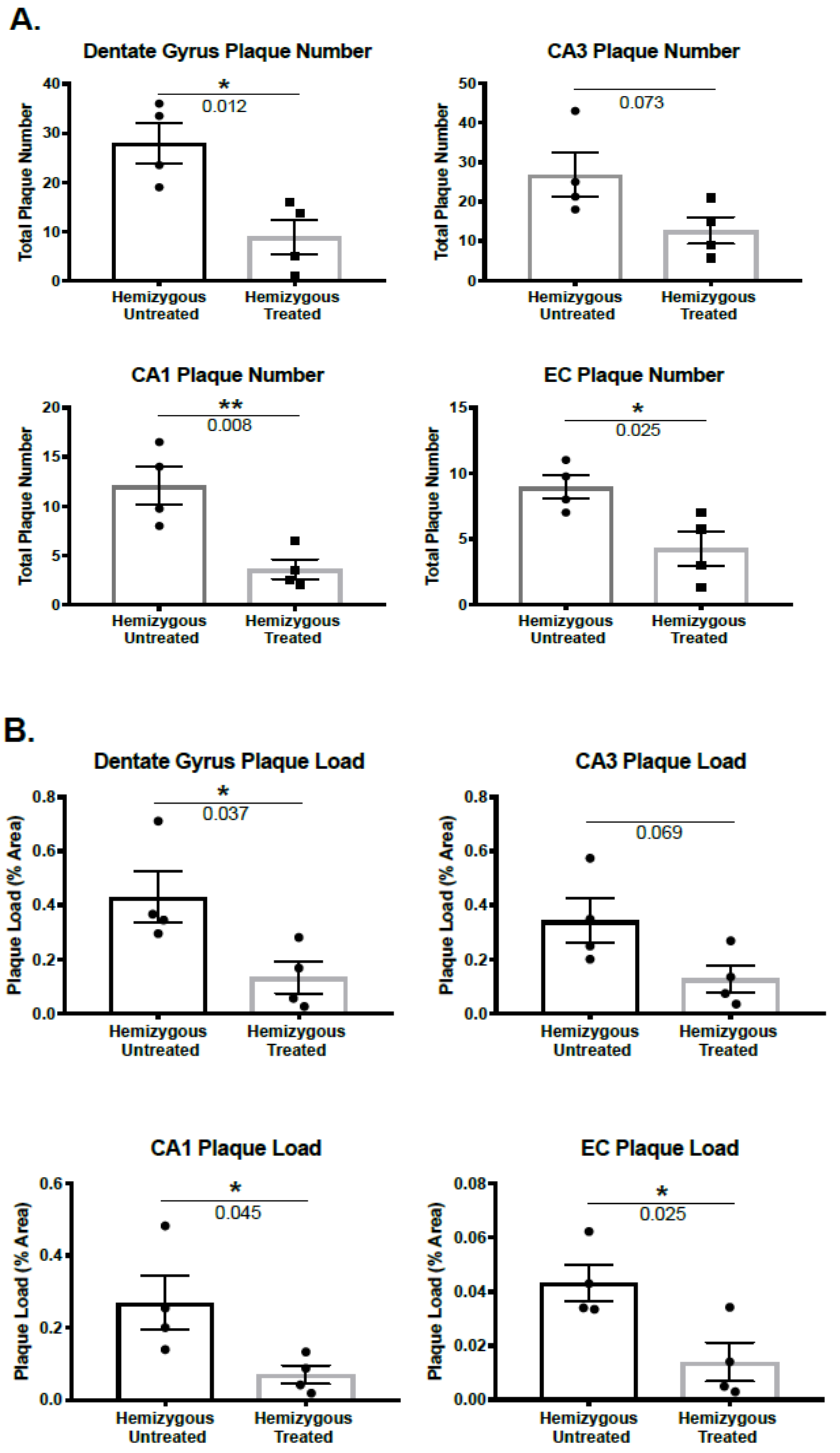

Fig 13. Quantification of amyloid plaque number and plaque load (A) amyloid plaque load (number of plaques/area) (B) for distinct regions of the hippocampus (dentate gyrus, CA3, CA1) and entorhinal cortex. Data expressed as mean±SEM, dots are individual subject means (n=4). *p<0.05, **p<0.01.

Chapter Four: Discussion

Reelin is a secretory glycoprotein that plays a role in the maintenance and regulation of LTP in neuronal synapses. Its sets a foundation for neuronal cells to be placed in right areas of the brain and continues to play a role in brain development through the lifetime of an individual. Therefore, its deficit can lead to severe debilitation of motor functions that finally affect involuntary activity. Addressing all the functions of reelin, especially those that are imperative in consolidation of neural network, we used cysteine-rich whey protein, Immunocal® for a fixed amount of time period and checked for resurgence/rescue of reelin in AD mouse model. Previous studies showed that Immunocal® elevate glutathione in the brain and spinal cord which acts as a neuroprotective agent from oxidative stress. This potential nutraceutical has been tested as a therapeutic source for schizophrenia and ALS mouse model (Ross et al., 2014; Song et al., 2017). From this study it was shown that, Immunocal® rescued reelin at the transcript and protein level in the prefrontal cortex of mouse model of schizophrenia. However, in AD patients, it is known that neuronal population of reelin secretory cells of Entorhinal cortex is most vulnerable to neurodegeneration. Therefore, we designed the experiment to first observe the site of synthesis in hippocampal region of mouse brains in the wild type and AD model. Consequently, we sought to evaluate the effects of Immunocal® on Reelin expression and signaling *in vitro* in hippocampal-entorhinal cortex rat brain slices and *in vivo* in the $hAPP_{SweInd}$ mutant (J20) mouse model of AD. Previous

work has shown that deficits in Reelin expression and/or Reelin signaling play a pathogenic role in several nervous system disorders including schizophrenia and AD. Thus, strategies aimed at correcting these deficits might provide a novel therapeutic approach to these devastating diseases. The cysteine-rich, whey protein supplement, Immunocal®, has previously been shown to elevate glutathione in the brain and spinal cord and is neuroprotective and therapeutically efficacious in mouse models of schizophrenia and amyotrophic lateral sclerosis (Ross et al., 2014; Song et al., 2017). Most recently, Immunocal® treatment has been shown to rescue Reelin expression at the mRNA and protein level in the prefrontal cortex of a mouse model of schizophrenia (Song et al., 2017). Given that Reelin expressing neurons of the entorhinal cortex layer II are a highly vulnerable population of cells that are lost very early in AD, we sought to evaluate the effects of Immunocal® on Reelin expression and signaling *in vitro* in hippocampal-entorhinal cortex rat brain slices and *in vivo* in the $hAPP_{SweInd}$ mutant (J20) mouse model of AD.

We evaluated the effects of Immunocal® treatment *in vivo* by treating hemizygous J20 AD mice from 3 months-old to 12 months-old. We assessed Reelin expression and signaling by western blotting and immunofluorescence microscopy. Immunocal® treatment corrected a deficit in cortical GSH levels observed in the brains of untreated hemizygous J20 mice. Western blotting of brain sections micro-dissected to enrich for the hippocampal-entorhinal cortex sub-region revealed a decrease in Reelin expression in untreated hemizygous J20 AD mice compared to non-carrier control mice. These deficits were corrected by treatment with Immunocal®. We evaluated Reelin transcript levels in hippocampal region of brain by in situ hybridization and quantified transcript levels by measuring total fluorescence intensity.

In order to probe for hippocampal specific regions of reelin expression, we used immunofluorescence microscopy technique. Reelin expression was diminished in the entorhinal cortex, dentate gyrus and CA1/CA3 regions of the hippocampus in untreated hemizygous J20 AD mice compared to non-carrier control mice. In contrast, Immunocal® treatment largely rescued these deficits in Reelin expression and in entorhinal cortex and dentate gyrus significantly. Since reelin is a secreted glycoprotein, it was observed to be present in all regions of hippocampus as seen in non-carrier mice. Therefore, we used insitu mRNA hybridization technique to investigate specific regions of hippocampus that synthesize reelin transcripts. Entorhinal cortex, CA3 and dentate gyrus of hippocampus were the only regions that expressed reelin transcripts. Due to tissue integrity being lost during slicing procedure in dentate gyrus, we assessed transcript levels only in CA3 and entorhinal cortex. There was a significant reduction in transcript expression in heterozygous untreated sample when compared with non-carrier. However, there was a significant rescue in mRNA levels in entorhinal region of Immunocal® treated sample. We suspect that entorhinal region may be involved in production of reelin through which other regions of hippocampal receive signal from trisynaptic pathway that is involved in long term potentiation.

Perhaps most importantly in the context of AD, we evaluated the deposition of amyloid plaques in the J20 mice. These mice have been shown to have significant plaque load at 12-month-old. We have shown that untreated J20 mice do indeed accumulate a significant plaque load in the hippocampus and entorhinal cortex. After treatment with Immunocal® the plaque load was diminished quite dramatically, both in size and number.

Chapter Five: Future direction and potential mechanism

The mice model used in this study only forms one of the pathological characteristics of Alzheimer's disease that is, Aβ plaques. In order to capitulate complete disease state, it would be interesting to use a mice model that also forms tangle pathology such as those seen in 3XTg-AD. Using this model may provide cues to reelin downstream signaling pathway. We would also like to probe for inflammatory response which could serve as an indicative of oxidative stress and cell injury in J20 as well as 3XTg-AD model by staining for microglial and astrocyte markers.

Based on these preliminary results, we have postulated a mechanism that may work towards reduction of pathological characteristics in AD. If Immunocal® treatment is initiated early-on, it increases glutathione levels in neuronal cells which decreases the excessive reactive oxidative species (ROS) generated through aging process. In a preliminary study from our lab, Immunocal® treatment was tested from 3-month old to 5-month old mice. In one of the experiments, we used transcription regulator p-CREB to test modulation of reelin synthesis. This transcriptional element is found upstream of reelin gene and maybe repressed under oxidative stress condition. We performed western blotting to observe p-CREB levels in control, untreated hemizygous J20 mice model and treated J20 mice model. The untreated hemizygous J20 AD mice displayed a marked reduction in p-CREB immunoreactivity in the hippocampal-entorhinal cortex sub-region of the brain and this deficit was essentially rescued by treatment with Immunocal®. With this we postulate that p-CREB maybe involved in activation of reelin levels in the cell.

Therefore, reelin levels increase in response to an increase in glutathione levels. As documented in this study, augmentation of reelin can decrease pathological effects in AD such as Aβ plaques and tau fibrils.

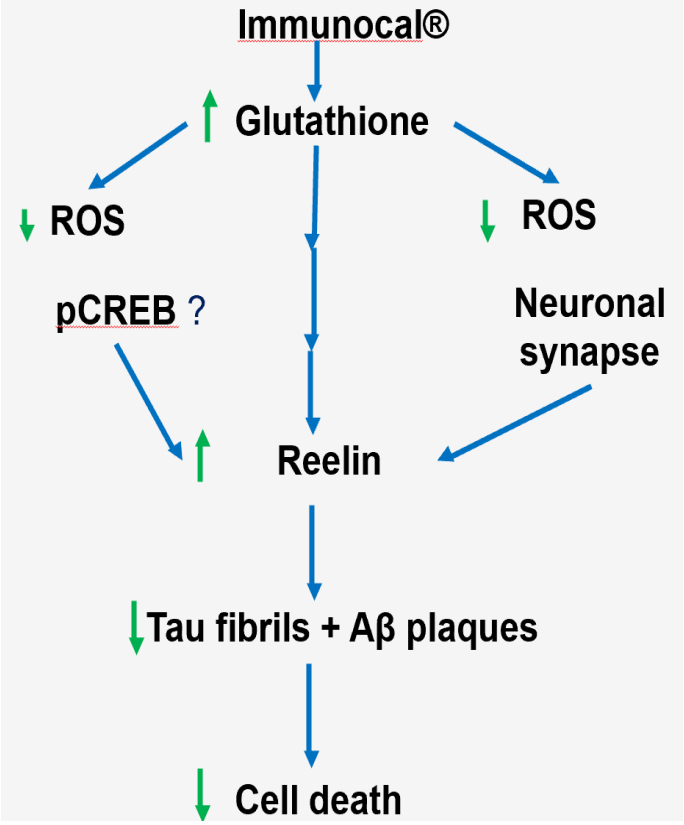

Figure 14: Potential mechanism of Immunocal® as a therapeutic in AD

References

(2017) Alzheimer's and Dementia, 13 (4), pp. 325-373

Amaral, D; Lavenex P (2006). "Ch 3. Hippocampal Neuroanatomy". In Andersen P; Morris R; Amaral D; Bliss T; O'Keefe J (eds.). The Hippocampus Book. Oxford University Press.

Andersen, P; Soleng AF; Raastad M (2000). "The hippocampal lamella hypothesis revisited". Brain Res.

Beffert,U., Weeber, E.J., Durudas, A., Qiu, S., Masiulis ,I., Sweatt, J.D., et al. (2005). Modulation of synaptic plasticity and memory by Reelin involves differential splicing of the lipoprotein receptor ApoER2. Neuron 47, 567–579

Bock, H. H., & May, P. (2016). Canonical and Non-canonical Reelin Signaling. Frontiers in cellular neuroscience.

Bosch, C., N. Masachs, D. Expsosito-Alsonso, A. Martínez, C. M. Teixeira, I. Fernaud, L. Pujadas, F. Ulloa, J. X. Comella, J. DeFelipe, A. Merchán-Pérez, E. Soriano (2016). “Reelin regulates the maturation of dendritic spine, synaptogenesis and glial ensheathment of newborn granule cells.” Cereb Cortex 26(11): 4282-4298

Bounous G., Gold P. The biological activity of undenatured dietary whey proteins: role of glutathione. Clinical and Investigative Medicine. 1991; 14:296–309

Cacace, R., Sleegers, K. & Van Broeckhoven, C.Molecular genetics of early-onset Alzheimer’s disease revisited. Alzheimers Dement. 12, 733–748 (2016).

Chin, J., C. M. Massaro, J. J. Palop, M. T. Thwin, G. Q. Yu, N. Bien-Lv, A. Bender, L. Mucke (2007). “Reelin depletion in the entorhinal cortex of human amyloid precursor protein transgenic mice and humans with Alzheimer’s disease.” J Neurosci 27(11): 2727-2733.

Cuchillo-Ibañez, I., V. Balmaceda, T. Mata-Balaguer (2016). “Reelin in Alzheimer’s disease, increased levels but impaired signaling: when more is less.” J Alz Dis 52: 403-416.

D’Arcangelo,G., Miao, G.G., Chen, S.C., Soares, H.D., Morgan, J.I., and Curran, T.(1995). A protein related to extra cellular matrix proteins deleted in the mouse mutant reeler. Nature 374, 719–723.doi:10.1038/374719a0

D’Arcangelo,G., Nakajima,K., Miyata,T., Ogawa,M., Mikoshiba,K., and Curran,T.(1997). Reelin is a secreted glycoprotein recognized by the CR-50 monoclonal antibody. J. Neurosci. 17, 23–31.

Del Turco, D. et al. Region-specific differences in amyloid precursor protein expression in the mouse hippocampus. Front. Mol. Neurosci. 9, 134 (2016).

Diaz-Hernandez, J. I., R. Gomez-Villafuertes, M. León-Otegui, L. Hontecillas-Prieto, A. Del Puerto, J. L. Trejo, J. J. Lucas, J. J. Garrido, J. Gualix, M. T. Miras-Portugal, M. Diaz-Hernandez (2012). “In vivo P2X7 inhibition reduces amyloid plaques in Alzheimer’s disease through GSK3β and secretases.” Neurobiol Aging 33(8): 1816-1828.

DiLoreto, R., & Murphy, C. T. (2015). The cell biology of aging. *Molecular biology of the cell*, *26*(25), 4524–4531.

D'Onofrio, G., F. Panza, V. Frisardi, V. Solfrizzi, B. P. Imbimbo, G. Paroni, L. Cascavilla, D. Seripa, A. Pilotto (2012). "Advances in the identification of gamma-secretase inhibitors for the treatment of Alzheimer's disease." Expert Opin Drug Discov 7(1): 19-37.

Evin, G., M. F. Sernee, C. L. Masters (2006). "Inhibition of gamma-secretase as a therapeutic intervention for Alzheimer's disease: prospects, limitations and strategies." CNS Drugs 20(5): 351-372

Falconer DS (January 1951). "Two new mutants, 'trembler' and 'reeler', with neurological actions in the house mouse (Mus musculus L.)" Journal of Genetics.

Gabriella D'Arcangelo, "Reelin in the Years: Controlling Neuronal Migration and Maturation in the Mammalian Brain," Advances in Neuroscience, vol. 2014, Article ID 597395, 19 pages, 2014.

Grey V., Mohammed S. R., Smountasm A. A., Bahlool R., Lands L. C. Improved glutathione status in young adult patients with cystic fibrosis supplemented with whey protein. Journal of Cystic Fibrosis. 2003; 2:195–198. doi: 0.1016/S1569-1993(03)00097-3

Hardy, J. A., G. A. Higgins. (1992). "Alzheimer's disease: the amyloid cascade hypothesis." Science 256(5054):184-185.

Held P. An introduction to reactive oxygen species: measurement of ROS in cells BioTek Instruments, Inc.: Winooski, VT; 2012

Herring, A., A. Donath, K. M. Steiner, M. P. Widera, S. Hamzehian, D. Kanakis, K. Kolble, A. El Ali, D. M. Hermann, W. Paulus W, K. Keyvani (2012). "Reelin depletion is an early phenomenon of Alzheimer's pathology." J Alz Dis 30(4): 963-979.

Hippius, H., & Neundörfer, G. (2003). The discovery of Alzheimer's disease. Dialogues in clinical neuroscience, 5(1), 101–108.

Hoe, H. S., Lee, K. J., Carney, R. S., Lee, J., Markova, A., Lee, J. Y., Markova A., Lee J., Howell B.W., Hyman B.T., Pak D.T.S., Bu G, Rebeck, G. W. (2009). Interaction of reelin with amyloid precursor protein promotes neurite outgrowth. The Journal of Neuroscience.

Hong, S.E., Shugart, Y.Y., Huang,D.T., Shahwan, S.A., Grant, P.E., Hourihane, J.O.,et al.(2000). Autosomal recessive lissencephaly with cerebellar hypoplasia is associated with human RELN mutations. Nat. Genet.

Jossin, Y.,and Goffinet ,A.M.(2007). Reelin Signals through phosphatidylinositol 3-kinase and Akt to control cortical development and through mTor to regulate dendritic growth. Mol. Cell.Biol. 27, 7113–7124.doi:10.1128/mcb.00928-07

Karl, T., S. Bhatia, D. Cheng, W. S. Kim, B. Garner (2012). "Cognitive phenotyping of amyloid precursor protein transgenic J20 mice." Behav Brain Res 228(2): 392-397.

Karran, E., B. De Strooper (2016). "The amyloid cascade hypothesis: are we poised for success or failure?" J Neurochem 139 Suppl 2: 237-252.

Kennedy M.E., Andrew W. Stamford, Xia Chen, Kathleen Cox, Jared N. Cumming, Marissa F. Dockendorf, Michael Egan, Larry Ereshefsky, Robert A. Hodgson, Lynn A. Hyde, Stanford Jhee, Huub J. Kleijn, Reshma Kuvelkar, Wei Li, Britta A. Mattson, Homg

Mei, John Palcza, Jack D. Scott, Michael Tanen, Matthew D. Troyer, Jack L. Tseng, Julie A. Stone, Eric M. Parker, Mark S. Forman (2016). The BACE1 inhibitor verubecestat (MK-8931) reduces CNS β-amyloid in animal models and in Alzheimer's disease patients. Science Translational Medicine 02 Nov 2016 : 363RA150

Kim, G. H., Kim, J. E., Rhie, S. J., & Yoon, S. (2015). The Role of Oxidative Stress in Neurodegenerative Diseases. Experimental neurobiology.

Kim, M., Jeong, Y., and Chang, Y.C. (2015). Extra cellular matrix protein reelin regulate dendritic spine density through CaMKIIb. Neurosci. Lett. 599, 97–101. doi: 10.1016/j.neulet.2015.05.033

Kobro-Flatmoen, A., A. Nagelhus, M. P. Witter (2016). "Reelin-immunoreactive neurons in entorhinal cortex layer II selectively express intracellular amyloid in early Alzheimer's disease." Neurobiol Dis 93: 172-183.

Kocherhans, S., A. Madhusudan, J. Doehner, K. S. Breu, R. M. Nitsch, J. M. Fritschy, I. Knuesel (2010). "Reduced Reelin expression accelerates amyloid-beta plaque formation and tau pathology in transgenic Alzheimer's disease mice." J Neurosci 30(27): 9228-9240

Koie, M.,Okumura,K.,Hisanaga,A.,Kamei,T.,Sasaki,K.,Deng,M.,etal. (2014). Cleavage within Reelin repeat 3 regulates the duration and range of the signaling activity of Reelin protein. J. Biol.Chem. 289, 12922–12930.doi:10.1074/jbc.M113.536326

Krstic, D., S. Pfister, T. Notter, I. Knuesel (2013). "Decisive role of Reelin signaling during early stages of Alzheimer's disease." Neuroscience 246: 108-116.

Kupferman J. V., Basu J., Russo M. J., Guevarra J., Cheung S. K., Siegelbaum S. A. (2014). Reelin signaling specifies the molecular identity of the pyramidal neuron distal dendritic compartment. Cell 158, 1335–1347. 10.1016/j.cell.2014.07.035

Lamber de Rouvroit, C., and Goffinet, A.M. (1998).The reeler mouse as a model of brain development. Adv. Anat. Embryol. CellBiol.

Lee, G. H., & D'Arcangelo, G. (2016). New Insights into Reelin-Mediated Signaling Pathways. Frontiers in cellular neuroscience, 10, 122. doi:10.3389/fncel.2016.00122

L. Mucke. Alzheimer's disease. Nature 461, 895–897 (2009).

Mani S. Production of reactive oxygen species and its implication in human diseases. In: Rani V, Yadav UC, editors. Free radicals in human health and disease. New Delhi: Springer; 2015.

Menting, K. W., & Claassen, J. A. (2014). β-secretase inhibitor; a promising novel therapeutic drug in Alzheimer's disease. Frontiers in aging neuroscience, 6, 165. doi:10.3389/fnagi.2014.00165

Mucke, L., E. Masliah, G. Q. Yu, M. Mallory, E. M. Rockenstein, G. Tatsuno, K. Hu, D. Kholodenko, K. Johnson-Wood, L. McConlogue (2000). "High-level neuronal expression of Aβ1-42 in wild-type human amyloid protein precursor transgenic mice: synaptotoxicity without plaque formation." J Neurosci 20(11): 4050-4058

Mullard A. (2017) "BACE inhibitor bust in Alzheimer trial." Nature Reviews Drug Discovery volume 16, page 155 (2017)

Müller T., H. E. Meyer, R. Egensperger, K. Marcus (2008). “The amyloid precursor protein intracellular domain (AICD) as modulator of gene expression, apoptosis, and cytoskeletal dynamics-relevance for Alzheimer’s disease.” Prog Neurobiol 85(4): 393-406

Niu, S.,Yabut,O.,andD’Arcangelo,G.(2008).The Reelin signaling pathway promotes dendritic spine development in hippocampal neurons. J. Neurosci. 28, 10339–10348.doi:10.1523/JNEUROSCI.1917-08.2008

Ogawa, M.,Miyata,T.,Nakajima,K.,Yagyu,K.,Seike,M.,Ikenaka,K.,etal.(1995). The reeler gene-associated antigen on Cajal-Retzius neurons is a crucial molecule for laminar organization of cortical neurons. Neuron 14, 899–912.

Pesold, C., Impagnatiello, F., Pisu, M.G., Uzunov, D.P., Costa, E., Guidotti, A., et al (1998). Reelin is preferentially expressed in neurons synthesizing g-aminobutyricacid in cortex and hippocampus of adult rats. Proc. Natl. Acad. Sci. USA 95, 3221–3226.doi:10.1073/pnas.95.6.3221

Pujadas, L., D. Rossi, R. Andrés, C. M. Teixeira, B. Serra-Vidal, A. Parcerisas, R. Maldonado, E. Giralt, N. Carulla, E. Soriano (2014). “Reelin delays amyloid-beta fibril formation and rescues cognitive deficits in a model of Alzheimer’s disease.” Nat Commun 5: 3443.

Ross, E. K., A. N. Winter, H. M. Wilkins, W. A. Sumner, N. Duval, D. Patterson, D. A. Linseman (2014). “A cystine-rich whey supplement (Immunocal®) delays disease onset and prevents spinal cord glutathione depletion in the hSOD1(G93A) mouse model of amyotrophic lateral sclerosis.” Antioxidants 3(4): 843-865

Sato, Y., Kobayashi, D., Kohno, T., Kidani, Y., Prox, J., Becker-Pauly, C., et al (2016). Determination of cleavage site of Reelin between its sixth and seventh repeat and contribution of meprin metalloproteases to the cleavage. J. Biochem.159, 305–312.doi:10.1093/jb/mvv102

Singh, S. K., Srivastav, S., Yadav, A. K., Srikrishna, S., & Perry, G. (2016). Overview of Alzheimer's Disease and Some Therapeutic Approaches Targeting Aβ by Using Several Synthetic and Herbal Compounds. Oxidative medicine and cellular longevity, 2016, 7361613. doi:10.1155/2016/7361613

Song P, Zou MH. (2015) Roles of reactive oxygen species in physiology and pathology. In: Wang H, Patterson C, editors. Atherosclerosis: risks, mechanisms, and therapies

Song, W., A. Tavitian, M. Cressatti, C. Galindez, A. Liberman, H. M. Schipper (2017). “Cysteine-rich whey protein isolate (Immunocal®) ameliorates deficits in the GFAP.HMOX1 mouse model of schizophrenia.” Free Radic Biol Med 110: 162-175.

Swerdlow R. H., S. Koppel, I. Weidling, C. Hayley, Y. Ji, H. M. Wilkins (2017). “Mitochondria, cybrids, aging, and Alzheimer’s Disease.” Prog Mol Biol Transl Sci 146: 259-302.

Tse K. H., K. Herrup (2017). “Re-imagining Alzheimer’s disease – the diminishing importance of amyloid and a glimpse of what lies ahead.” J Neurochem epub ahead of print.

Vassar, R. (2001). "The beta-secretase, BACE: a prime drug target for Alzheimer's disease." J Mol Neurosci 17(2): 157-170.

Vassar, R., Kovacs, D. M., Yan, R., & Wong, P. C. (2009). The beta-secretase enzyme BACE in health and Alzheimer's disease: regulation, cell biology, function, and therapeutic potential. The Journal of neuroscience : the official journal of the Society for Neuroscience, 29(41), 12787–12794. doi:10.1523/JNEUROSCI.3657-09.2009

Wasser, C. R., J. Herz (2017). “Reelin: neurodevelopmental architect and homeostatic regulator of excitatory synapses.” J Biol Chem 292(4): 1330-1338.

Weeber, E.J., Beffert, U., Jones, C., Christian, J.M., Forster, E., Sweatt, J.D., et al (2002). Reelin and ApoE receptors cooperate to enhance hippocampal synaptic plasticity and learning. J. Biol.Chem. 277, 39944–39952.doi:10.1074/jbc.m205147200

Wilson, R. S., Segawa, E., Boyle, P. A., Anagnos, S. E., Hizel, L. P., & Bennett, D. A. (2012). The natural history of cognitive decline in Alzheimer's disease. Psychology and aging, 27(4), 1008–1017.

Winter, A. N., Ross, E. K., Daliparthi, V., Sumner, W. A., Kirchhof, D. M., Manning, E., Heather M. Wilkins, Linseman, D. A. (2017). A Cystine-Rich Whey Supplement (Immunocal®) Provides Neuroprotection from Diverse Oxidative Stress-Inducing Agents In Vitro by Preserving Cellular Glutathione. Oxidative medicine and cellular longevity, 2017, 3103272. doi:10.1155/2017/3103272

Yu N. N., M. S. Tan, J. T. Yu, A. M. Xie, L. Tan (2016). “The role of reelin signaling in Alzheimer’s disease.” Mol Neurobiol 53(8): 5692-5700.

Zitka, O. et al., (2012). Redox status expressed as GSH:GSSG ratio as a marker for oxidative stress in paediatric tumour patients. *Oncology letters*, *4*(6), 1247–1253. doi:10.3892/ol.2012.931

Zorov D.B., Juhaszova M, Sollott SJ. Mitochondrial reactive oxygen species (ROS) and ROS-induced ROS release. Physiol Rev. 2014;94:909–950

Appendix: Abbreviations

AD: Alzheimer's disease
AKT: Protein kinase B also known as AKT
APC: Antigen presenting Cell
ApoER2: Apolipoprotein E receptor-2
APP: Amyloid precursor protein
hAPP: human Amyloid precursor protein
ANOVA: Analysis of variance
BACE: β secretase
BCA: Bicinchoninic acid assay
BSA: Bovine serum albumin
CDC: cell cycle division
CA: Cornus Ammonis
CAT: catalase
CR: Cajal Retzius
Ct: C-terminal
Cy3: Cyanine-3 conjugated
DAB1: Disabled-1
DG: Dentate gyrus
EC: Entorhinal cortex
ER: Endoplasmic reticulum
FITC: Fluorescein Isothiocyanate conjugated
Fyn: Proto-oncogene tyrosine-protein kinase fyn
GABA: gamma-aminobutyric acid
γ -GCS: γ-glutamyl synthetase
GAD: Glutamate decarboxylase
GS: Glutathione synthetase
GPx: Glutathione peroxidase
GSH: Glutathione
GSSG: Glutathione disulphide
HPLC-ECD: High performance liquid chromatography and electro-chemical detection
HRP: Horseshoe radish peroxide
HSV: Hue, saturation, lightness
KOH: Potassium hydroxide
LTP: Long term potentiation
PAK: Serine/threonine-protein kinase
PBS: Phosphate buffered solution
PFA: Para formaldehyde
PI3k: Phosphoinositide 3-kinase
PS1: presenilin 1
PS2: presenilin 2
PVDF: Polyvinylidene difluoride
NADPH: Nicotinamide adenine dinucleotide phosphate
Nox: NADPH oxidase
NOS : Nitric oxide synthase
NMDA: N-methyl-D-aspartate receptor
Nt: N-terminal
ROS: Reactive Oxygen Species

R: Repeats
SDS-PAGE: Sodium dodecyl sulfate-Polyacrylamide gel electrophoresis
S.E.M. : Standard error of the mean
SOD: Superoxide dismutase
Src: Proto-oncogene tyrosine-protein kinase src
SweInd: Swedish Indiana mutant
VLDLR: very low density lipoprotein receptor
XO: xanthine oxidase